

SpChar: Characterizing the Sparse Puzzle via Decision Trees

Francesco Sgherzi^{a,b,*}, Marco Siracusa^{a,b}, Ivan Fernandez^{a,b}, Adrià Armejach^{a,b}, Miquel Moretó^{a,b}

^aBarcelona Supercomputing Center, Plaça d'Eusebi Güell, 1-3, Barcelona, 08034, Spain

^bUniversitat Politècnica de Catalunya, Carrer de Jordi Girona, 31, Barcelona, 08034, Spain

Abstract

Sparse matrix computation is crucial in various modern applications, including large-scale graph analytics, deep learning, and recommender systems. The performance of sparse kernels varies greatly depending on the structure of the input matrix, making it difficult to gain a comprehensive understanding of sparse computation and its relationship to inputs, algorithms, and target machine architecture. Despite extensive research on certain sparse kernels, such as Sparse Matrix-Vector Multiplication (SpMV), the overall family of sparse algorithms has yet to be investigated as a whole. This paper introduces SpChar, a workload characterization methodology for general sparse computation. SpChar employs tree-based models to identify the most relevant hardware and input characteristics, starting from hardware and input-related metrics gathered from Performance Monitoring Counters (PMCs) and matrices. Our analysis enables the creation of a *characterization loop* that facilitates the optimization of sparse computation by mapping the impact of architectural features to inputs and algorithmic choices. We apply SpChar to more than 600 matrices from the SuiteSparse Matrix collection and three state-of-the-art Arm CPUs to determine the critical hardware and software characteristics that affect sparse computation. In our analysis, we determine that the biggest limiting factors for high-performance sparse computation are (1) the latency of the memory system, (2) the pipeline flush overhead resulting from branch misprediction, and (3) the poor reuse of cached elements. Additionally, we propose software and hardware optimizations that designers can implement to create a platform suitable for sparse computation. We then investigate these optimizations using the gem5 simulator to achieve a significant speedup of up to 2.63× compared to a CPU where the optimizations are not applied.

Keywords: Sparse Computation, Workload Characterization, Arm,

*Corresponding author

Email addresses: francesco.sgherzi@bsc.es (Francesco Sgherzi), marco.siracusa@bsc.es (Marco Siracusa), ivan.fernandez@bsc.es (Ivan Fernandez), adria.armejach@bsc.es (Adrià Armejach), miquel.moreto@bsc.es (Miquel Moretó)

1. Introduction

Operating with sparse matrices is crucial for many of today’s applications. Kernels like Sparse Matrix-Vector Multiplication (SpMV), Sparse General Matrix-Matrix Multiplication (SpGEMM), and Sparse Matrix Addition (SpADD) are the building blocks for Recommender Systems [1], Ranking [2], Genomics [3] and, more broadly, serve as a proxy for the operations performed in the more broader Sparse Tensor Algebra field [4]. Moreover, as ever bigger Language Models [5] and Latent Diffusion Models [6] enter mass adoption, it has become apparent that both training and deploying *dense* models incur in extremely high machinery and energy costs [7, 8], as well as hindering the ability to deploy such models on-edge rather than in a data center. In this scenario, Neural Network sparsification has been proven effective in reducing energy and time requirements for training and inference [9, 10, 11, 12].

Sparse workloads exhibit diverse memory access patterns and arithmetic intensities, which vary greatly across kernels as well as inputs, thereby making input characterization crucial to determine the requirements for a platform to excel in sparse computation. On a fundamental level, Sparse kernels greatly benefit from high bandwidth memories in conjunction with low latency memories, as most of them exhibit a scan-and-lookup access pattern [13]. However, memory systems typically fail to deliver the stringent bandwidth and latency demands of sparse workloads. For this reason, the available compute throughput is hindered by the memory system [14], thus requiring complex prefetching mechanisms [15], and large caches to better utilize the core’s arithmetic capabilities.

Orthogonally, determining the impact of a certain architectural feature (e.g., size of Miss Status Holding Register (MSHR), memory technology, number of cores) on an kernel applied to a given input is crucial in sectors that employ matrices of specific kinds, which is the case in the fields of structural engineering, social network mining and sparse neural networks. In this setting, a promising approach that is gaining traction is the use of Machine Learning (ML) models [16, 17] to estimate the performance and impact of an architectural change quickly, in contrast to more accurate but slower simulation-based approaches [18, 19].

While performance characterization of some sparse kernels, namely SpMV, has been thoroughly explored [20, 21, 22, 23], the problem of choosing an appropriate architecture for sparse computation (hereafter referred as *sparse problem*) has yet to be tackled as a whole, even if other sparse kernels like SpADD or SpGEMM are fundamental operations for the broader tensor algebra field. Moreover, recent work that characterizes those kernels mostly focuses on a single architecture and a single kernel, while only employing limited sets of matrices to carry the evaluation forward. As a result, architectural insights on sparse computation are hard to obtain due to the interdependence of architecture, inputs,

and kernels in this category of heavily data-dependent problems.

SpChar is the first to tackle the *sparse problem* from a holistic point of view. Specifically, our goal is to create a new analysis method to establish a *characterization loop* that enables hardware and software designers to map the impact of architectural features to algorithmic choices and input, and then optimize from the insights gathered. To this end, we gather matrices from 9 different domains, and we statically characterize (i.e., without running any sparse kernels) them based on the impact they have on certain architectural features (e.g., ease of branch prediction, randomness of the resulting access pattern, imbalance when partitioned on multiple threads). We use them to benchmark SpMV, SpGEMM, and SpADD on 3 different Arm platforms and profile the executions using Performance Monitoring Counters (PMCs) via the `perf` suite. We then feed both the matrix metrics and a subset of the PMCs to a Decision Tree Regressor and extract the most relevant splitting attributes. By comparing splitting attributes across Central Processing Units (CPUs) we can see the impact of architectural choices and inputs on a given kernel. In our analysis, we show that (1) SpMV is bottlenecked by the latency of the memory system when inputs show low locality and by the overhead of pipeline flushes due to branch mispredictions, (2) SpGEMM is bottlenecked by continuous cache evictions as a result of poor reuse of the values of the right-hand side matrix, and (3) SpADD is bottlenecked by the branch misprediction overhead and is less dependent on the underlying matrix structure.

In summary, this paper presents the following contributions:

- We present SpChar: a workload characterization methodology for Sparse computation that considers both the hardware perspective and the input perspective. We employ tree-based models determine what are the most impactful CPU features (e.g., size of the Last Level Cache (LLC), memory technology) for a given a combination of kernel and input.
- We evaluate our methodology on a set of 600 matrices spanning 9 different domains (e.g., structural engineering, social networks) using 3 different ARMv8 CPUs on 3 sparse kernels.
- We explore a practical application of SpChar within a software-hardware characterization loop. To this end, we assess the effectiveness of our proposed optimizations on the SpMV kernel, executed on a simulated Arm platform. Our proposed optimizations are effective in reducing the execution time and increasing throughput of SpMV, with a speedup of up to $2.63\times$ compared to a CPU where such optimizations are not applied.

2. Background and Motivation

2.1. Sparse Formats and Kernels

This section introduces the sparse formats and kernels we selected to study sparse computation. As sparse linear-algebra libraries are less mature compared

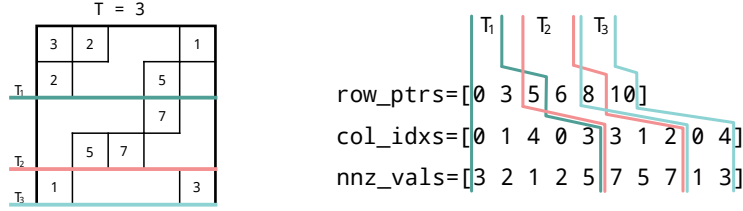


Figure 1: Row-wise partitioning scheme for Compressed Sparse Row (CSR) on 3 threads. Each thread operates on the contiguous set of rows displayed on the left, which translates to the *influence regions* on the right. Note that partitions of the `row_ptrs` array overlap because each thread requires knowing what is the index of the last element the previous thread operated on.

to their dense counterparts, we could only select three kernels with a single format. Moreover, we wanted to select simple-enough kernels that just contain few operations in order to study their performance impact in isolation.

2.1.1. The CSR format

Although there are many sparse formats in the literature, CSR [24, 25] is perhaps one of the most used [26]. As depicted in Figure 1, it is composed of three arrays:

- **nnz_vals**: stores the values of the non-zero entries of a matrix in row-major order.
- **col_idxs**: stores the column indexes of the non-zero entries of a matrix in row-major order.
- **row_ptrs**: stores the position of the first element of each row within the **nnz_vals** and **col_idxs** arrays.

Overall, CSR provides a good trade-off between storage efficiency and versatility. In fact, the **row_ptrs** vector provides direct row indexing, which is essential in certain dataflow algorithms (e.g., SpGEMM CSR [27]) and row-based work partitioning as shown in Figure 1.

2.1.2. The SpMV kernel

As detailed in Algorithm 1, SpMV [28] multiplies a sparse matrix with a dense vector and returns a dense vector. If the sparse matrix stores graph adjacencies, this nested-loop structure is a typical traversal operation that can be found in many graph algorithms that SpMV is the building block of (e.g. Pagerank, Breadth First Search, etc) [29].

When using CSR, thread parallelism is generally enforced row-wise on the outer loop whereas data parallelism is enforced element-wise in the inner loop [30]. On today’s processors, the most critical operation of this algorithm is the indirect access on the dense vector [31, 25]. If the access pattern has low spatio-temporal locality, elements are likely to be gathered from lower cache layers,

requiring longer-latency accesses that saturate the memory subsystem. Another important aspect is that the dependent nested-loop structure performing the matrix traversal introduces a row overhead that may harm performance on matrices with few non-zeros per row [32]. As indirect access and traversal of compressed sparse formats are common operations in sparse linear algebra and tensor-algebra kernels (e.g. SpMM [33], MTTKRP [34], etc), we believe SpMV is one of the most important proxies to study sparse computation.

2.1.3. The SpGEMM kernel

<hr/> Algorithm 1: SpMV CSR algorithm <hr/> <p>Data: $A \in \mathbb{R}^{p \times q}$, $x \in \mathbb{R}^q$ Result: $y \in \mathbb{R}^p$ $\triangleright A$ is a sparse matrix, y, x are dense vectors</p> <pre> for $a_{i*} \in A$ do for $a_{ij} \in a_{i*}$ do $y_i \leftarrow y_i + a_{ij} \times x_j$; end end </pre> <hr/>	<hr/> Algorithm 2: SpGEMM CSR algorithm <hr/> <p>Data: $A \in \mathbb{R}^{p \times q}$, $B \in \mathbb{R}^{q \times r}$ Result: $C \in \mathbb{R}^{p \times r}$ $\triangleright A, B, C$ are sparse matrices</p> <pre> for $a_{i*} \in A$ do for $a_{ij} \in a_{i*}$ do for $b_{jk} \in b_{j*}$ do $value \leftarrow a_{ij} \times b_{jk}$; if $c_{ik} \notin c_{i*}$ then $c_{ik} \leftarrow 0$; end $c_{ik} \leftarrow c_{ik} + value$; end end end </pre> <hr/>
--	--

SpGEMM multiplies two sparse matrices and returns a sparse matrix. This algorithm is of fundamental importance for linear algebra and graph analytics as is widely used for multigrid solvers, triangle counting, multi-source BFS, and others [35].

Although there are several versions of SpGEMM, we only consider the Gustavson’s implementation [27] reported in Algorithm 2, as the mostly used one [35]. Conversely from SpMV, SpGEMM also requires to build the output matrix that is generally generated in two phases: symbolic (firstly populates `row_ptrs` and allocates `col_idxs` and `nnz_vals`) and numeric (then computes and writes `col_idxs` and `nnz_vals`). In both cases, this algorithm sequentially traverses matrix A and indirectly accesses rows of matrix B , which are then accumulated and stored. We believe SpGEMM is an interesting test case as (1) the indirect access on matrix B has more spatial locality but less temporal locality than SpMV, stressing the memory subsystem in a different way and (2) the accumulation operation is of fundamental importance in sparse computation and is also used in higher-dimensional kernels such as sparse tensor contraction.

2.1.4. The SpADD kernel

SpADD adds two sparse matrices and returns a sparse matrix. As reported in Algorithm 3, the kernel iterates through the rows of the two matrices and

Algorithm 3: SpADD CSR algorithm

Data: $A \in \mathbb{R}^{p \times q}$, $B \in \mathbb{R}^{p \times q}$ **Result:** $C \in \mathbb{R}^{p \times q}$ **for** $a_{i*} \in A$ **and** $b_{i*} \in B$ **do** **merge (copy or sum)** a_{i*} **and** b_{i*} **until some row is fully scanned** **copy remaining elements in** a_{i*} **copy remaining elements in** b_{i*} **end**

merges them (copy if the given index is present in only one row, sum otherwise) if they both contain some non-zero element or just copies them otherwise [36]. In contrast to the other kernels, SpADD is not as memory intensive since the two CSR matrices are traversed sequentially. However, the disjunctive-merging operation is quite control intensive, particularly stressing Arithmetic Logic Units (ALUs) and branch predictors. Since merging operations — both in disjunctive and conjunctive mode — are quite common in higher-order tensor algebra (e.g. sparse tensor contraction) [37], we believe SpADD is a representative proxy to study the control overhead of sparse operations.

2.2. The case for Workload Characterization of Sparse Algorithms

In recent years, the application of sparse algorithms has evolved from being limited to scientific codes [38, 39, 40] and benchmarks [41, 42] to being ubiquitous in today’s workloads. With the rise of ever-bigger graphs representing social network topologies and more detailed user-buy-product characterizations for recommender systems, it is clear that sparse computation is gradually expanding to the cloud domain. Cloud providers like Google Cloud Platform (GCP), Amazon Web Services (AWS), Alibaba Cloud, and Oracle Cloud Infrastructure (OCI) already provide different CPUs to best suit the needs of their clients. With all of them now offering Arm alternatives to the more mainstream X86.64 machines and even building their own (i.e., Graviton series for AWS and Yitian 710 for Alibaba Cloud), the application domain of Arm architectures is expanding from mobile to High Performance Computing (HPC) and datacenters.

Now more than ever, algorithms operating on sparse matrices are employed in a plethora of domains, many of which share very few similarities. This discrepancy stems from sparse algorithms being vastly dependent on the underlying matrix structure in contrast to algorithms operating on dense matrices being generally input agnostic. Moreover, as we discuss in Section 2.1, the degree to which the performance of an algorithm depends on the input dramatically depends on the algorithm itself: algorithms like SpMV and SpGEMM are inherently more sensitive than SpADD.

In light of this, while architectural features to optimize dense arithmetic operations are well studied and characterized for CPUs [43, 44], Graphics Processing Units (GPUs) [45, 46], and Domain Specific Architectures (DSAs) [47, 48];

it is not immediately clear which are the design decision that would best benefit sparse computation. Traditionally, having higher Memory Level Parallelism (MLP) has made GPUs the *de facto standard* platform for sparse computation; however, higher memory latency [49] and smaller caches make them less applicable to workloads that operate on limited size matrices, like recommender systems [1] or graph clustering [50], with a possible solution being CPU-GPU co-computation [51]. In the scope of performance characterization of sparse workloads, while there exists an extensive body of work characterizing SpMV [52, 14, 20, 21, 22, 23, 53] and the structure of the inputs [54, 55, 56], SpADD and SpGEMM have historically received less attention, despite being relevant proxies for the operations performed in the broader tensor algebra field [57, 58, 59]. To this day, advancements in the algorithms above are mainly carried forward from the algorithmic side [60, 61, 62], with limited attention to the inputs' structure [63].

To the best of our knowledge, there exists no prior work characterizing several sparse matrix algorithms on different architectures that focuses deeply on the inputs' structure.

2.3. Mapping Architectural Features to Inputs and Algorithms

While ML methods are starting to gain traction in design space exploration and performance prediction, they are still not well established in the broader field of computer architecture. This is due to them having limited explainability (see Burkart et al. [64] and references therein), thus making the task of automatizing the gathering of architectural insights from the model parameters far from trivial. Exceptions to this rule are, among others [65, 66, 67, 68], tree-based models [69], which have seen adoption in hardware-software codesign [70, 71, 72].

In addition to being *more explainable*, tree-based models are paving the way for the use of ML in computer architecture due to being generally more resilient to the magnitude of the input features and fairly easy to use and deploy. Recent works have used tree-based models for performance prediction [73, 74] and automatic design space exploration [75, 76]. Within the scope of extracting relevant software/architectural insight from profiling, Fenacci et al. [77] employ decision trees to gather insights on benchmarks targeting embedded applications. Albeit focusing on the performance characterization of specific domains (e.g. networking, telecommunications, automotive), they employ only data derived by performance counters and do not take into account input-related metrics. As a result, while domains are characterized from the hardware perspective, seeing how workloads that are data-dependent react to the variation of inputs and how this interacts with hardware features is not achievable with this method. More recently Bang et al. [78] has used tree-based models to determine relevant features of IO-intensive workloads starting from logs generated from the top 20 apps executed on the CORI Supercomputer. As a result, the insights they gather are more focused on the general behavior of the suite of applications deployed on the supercomputer rather than on hardware characteristics.

Moreover, within the scope of extracting relevant hardware/software features from decision trees, one needs to exercise an abundance of caution when drawing the conclusion that some splitting attribute of the decision tree impacts the architecture in a relevant way, as these methods reflect the correlations present in the dataset rather than implying causality between features. As we later discuss in Section 3.5, one way to escape the correlation-implies-causation dilemma is to compare the relevant attributes from different models targeting the same features, analyze the presence (and absence) of features across models and ultimately link them to the known architectural choices for a given machine.

To the best of our knowledge, no prior work exists that uses decision trees to extract relevant hardware and input insights by comparing different architectures.

3. SpChar Methodology

3.1. Hardware and Algorithms

We profile and benchmark three state-of-the-art Arm platforms from both Cloud and HPC sectors: Fujitsu’s A64FX [79], Huawei’s Kunpeng 920 [80], and the more recent Graviton 3 [81] used on AWS. Such platforms are not only a good representation of the Arm ecosystem at the time of writing this paper, but they also have different memory technologies, as well as greatly different architectural design choices in terms of cache sizes, size of the vector units, and core count. Table 1 summarizes the most important features of the architectures under study and their system software.

Table 1: Summary of the architectural and software features of the CPUs

	A64FX	Kunpeng 920	Graviton 3
Manufacturer	Fujitsu	Huawei	Amazon
Architecture	ARM v8.2	ARM v8.2	ARM v8.4
Sockets	1	2	1
Cores per socket	48	64	64
Vector units	2×512 -bit SVE	1×128 -bit NEON	2×256 -bit SVE
L1D, L1I per core	64 kB, 64 kB	64 kB, 64 kB	64 kB, 64 kB
Private L2	N/A	64×512 kB	64×1 MB
Shared LLC	4×8 MB	64 MB	32 MB
Memory technology	HBM2	DDR4	DDR5
Memory channels	32	16	8
Peak bandwidth	1024 GB/s	380 GB/s	300 GB/s
Operating System	Red Hat Enterprise Linux 8.1	CentOS Linux 7	Ubuntu 22.04
Compiler	armclang 22.0.2	armclang 22.0.2	armclang 22.0.2
Kokkos Version	Kokkos 3.5	Kokkos 3.5	Kokkos 3.5

We benchmark SpMV, SpADD (Symbolic/Numeric), and SpGEMM (Symbolic/Numeric) kernels using single precision floating point for the `nnz_vals` vector and unsigned integers for the `row_ptrs` and the `col_idxs` vectors (4B wide in our systems). The kernels are provided by the Kokkos Kernels [82]

library, which we choose as it provides implementations that are vectorized both for NEON [83] (Kunpeng 920) and Scalable Vector Extension (SVE) [84] (A64FX and Graviton 3). For all input matrices, we run the specific kernel in two phases. First, we run the kernel J times without profiling it, which removes the effect of spinning up `OpenMP` threads and warms up hardware structures (e.g., caches). After the warmup phase, we run the kernel K times, profiling each run individually. In our experiments, we use $J = 10$ and $K = 5$, which strikes a balance between having profiling results with low variance across runs and having reasonable execution times. While Kokkos Kernels provides an implementation of SpMV that is *ready to use*, some options need to be tweaked for SpADD and SpGEMM. For starters, both algorithms need the `team_work_size` to be set, which refers to the number of fundamental operations (row sum for SpADD, row product for SpGEMM) that each thread is assigned per OpenMP batch. For our benchmarks, we set this value to 16, as it is the same value used by the authors of the library for performance regression testing in version 3.5. While higher values (e.g., 32, 128, 256) might yield better performance in matrices distributed with low imbalance across threads, it also decreases performance significantly in matrices with high imbalance. Choosing the optimal value requires *a priori* knowledge of the input matrix, and different architectures might perform optimally under distinct `team_work_size` parameters, even for the same matrix. As our goal is evaluating different architectures, we deem more relevant to choose sensible defaults rather than optimizing ad-hoc for each combination of matrix and architecture. Regarding SpGEMM, the library proposes several algorithmic choices. For our evaluation, we select the `KK.SPEED` version as it yields better performance at the cost of an higher memory usage.

While high-performance implementations of such algorithms are also present in the Arm Performance Libraries (ARMPL), the implementation of SpADD is not multithreaded and both SpADD and SpGEMM do not expose methods to execute the symbolic phase by itself. We release the code for this benchmarking suite and can be found at <https://gitlab.bsc.es/fsgherzi/spchar-benchmarking>.

We use the CSR matrix format [85], as it is widely employed and supported by several libraries [86, 87, 88, 89], including Kokkos. While a plethora of other sparse matrix formats do exist (e.g. COO, DCSR, ELL and variants), they are either (1) domain or architecture specific [1, 90], (2) could incur in wasteful data replication [91], or (3) require additional decompression at computation time [92]. CSR, on the other hand, is fairly agnostic of the matrix structure/domain, does not require decompressing data before being used, and opens itself to simple vectorization techniques.

3.2. Profiling Methodology

We select `perf` [93] as the profiling framework as it comes pre-packaged with most Linux distributions and is relatively easy to use. Operating with performance counters can be performed via plain syscalls (`perf_event_open`), which has streamlined the instrumentation of the benchmarks. Other profiling frameworks were considered (`likwid` [94], `papi` [95], `extrae` [96]) but later discarded due to either offering no additional functionality compared to `perf`,

being too fine-grained (trace-based profiling), offering aggregated metrics, or being more complex in usage within the scope of the instrumentation of the kernels. Nonetheless, profiling results were cross-referenced frequently to determine the correctness of the ad-hoc `perf` instrumentation.

Performance counter identifiers for architectures can be obtained from two distinct sources: the official Arm Performance Monitor Unit (PMU) reference and the CPU manufacturer optimization guides. The Arm PMU references contain counters that are core-related (e.g., frontend and backend stalls, core cache misses, scalar and vector floating point operations), whereas the counters provided by the manufacturers generally cover uncore architectural elements, such as the network-on-chip, last level caches, memory controllers and communication to memories and data exchanges across Non-Uniform Memory Access (NUMA) domains. In our analysis, we use the counters provided by the manufacturer reference optimization guides for A64FX and Kunpeng 920, whereas we use the Arm PMU reference for Graviton 3 as no document containing uncore counters is publicly available at the time of writing this document. The list of performance counters for each CPU can be found in Table 2.

Table 2: Summary of PMU counters for each CPU. **Counter ID** refers to the name used in the PMU reference manuals of A64FX, Kunpeng 920, Graviton 3.

	Counter ID	Supported CPU
Cycles elapsed	CPU_CYCLES	All
Executed Instructions	INST_RETIRED	All
Cycles stalled in frontend	STALL_FRONTEND	All
Cycles stalled in backend	STALL_BACKEND	All
Scalar fp instructions	VFP_SPEC	All
Vector fp instructions	ASE_SPEC	All
Load cacheline in L2	L2_CACHE_REFILL	A64FX
Store cacheline to memory	L2_CACHE_WB	A64FX
LLC Miss (L2)	L2_MISS_COUNT	A64FX
LLC Miss (L3)	L3_CACHE_MISS_RD	Kunpeng 920, Graviton 3
L1 Accesses	L1D_CACHE	All
Memory Accesses	MEM_ACCESS	Kunpeng 920, Graviton 3
Branch mispredicted	BR_MIS_PRED	All
Branch executed	BR_RETIRED	All

3.3. Datasets

The kernels are tested on the biggest 600 matrices by number of nonzero elements from the SuiteSparse Matrix collection [97]. These matrices have varying sizes ($\sim [10^6, 10^9]$ nonzeros) and densities ($\sim [10^{-7}\%, 25\%]$), and come from 9 different domains (e.g., computer vision, network problems, social networks), thus exhibiting different structures that are representative of real-world fields of applications. The biggest 600 matrices were chosen in order to prevent our

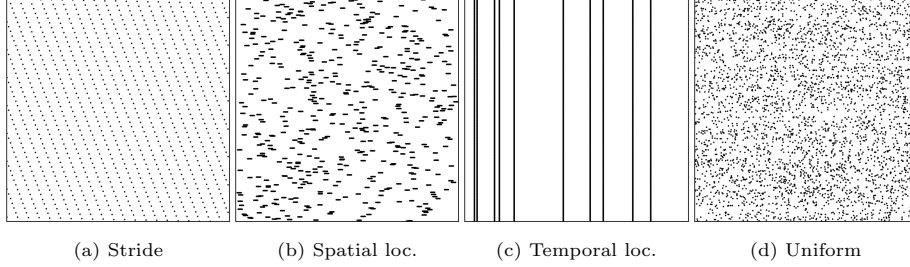


Figure 2: Four of our generation methods: we can generate matrices following several distributions of nonzeros and that stress specific architectural features.

CPUs to fully cache computational elements (e.g., right-hand side matrix in SpADD and SpGEMM, dense vector in SpMV) at any one time.

In addition to real-world matrices, we enrich our dataset with synthetic matrices, specifically generated to stress a particular CPU characteristic. Albeit the number of nonzero elements of each matrix varies depending on the generation method, the number of rows and columns is fixed at 16 million to impede the presence of computational elements like the dense vector (64 MB) for SpMV in the last-level cache.

Firstly, we test the impact of having an input with optimal spatial locality by adding a matrix comprised of a single dense row. On certain workloads (i.e., SpMV, SpADD) this generates a regular access pattern that allows elements to be prefetched easily. Conversely, to test optimal temporal locality and simple branch prediction, we use a matrix comprised of a single dense column. We then expand on this idea by including matrices that contain a cyclic pattern of nonzeros per row: this stresses the branch predictor in a controlled way, as the inner loops of SpMV, SpADD, and SpGEMM operate on the elements of a single row at a time.

To test the CPU’s prefetchers, we include matrices that present elements in a strided pattern (Figure 2a) in which contiguous nonzeros of the matrix appear at *cache_line_size*/4B intervals. To determine the impact of optimal spatial locality (Figure 2b), we generate matrices with elements in clusters of 10 elements, as it is an amount of nonzeros per row commonly found in literature [98, 99]. Conversely, to get optimal temporal locality (Figure 2c), we generate matrices whose non-zeros always appear in the same columns. Finally, we test the impact of several random distributions of nonzeros per row, typically found in real-world matrices such as scale-free graphs [100, 101, 102]. We achieve this by determining the number of nonzeros per row via uniform sampling of the inverse Cumulative Distribution Function (CDF) [103] of the Gaussian, Exponential, and Uniform (Figure 2d) distribution. Table 3 summarizes the 9 categories of synthetic matrices we generate, along with the feature they outline. The synthetic matrix generator is publicly available and can be found at <https://gitlab.bsc.es/fsgherzi/spchar-matrix-generator>.

Table 3: Synthetic matrices and their characteristics. The labels LOW, AVERAGE, HIGH refer to the a metric being below the first quartile (Q1), within the first and third quartile (Q1-Q3), and above the third quartile (Q3), respectively.

Category	Temporal Locality	Spatial Locality	Row Imbalance	Branch Entropy
Row	LOW	HIGH	HIGH	LOW
Column	HIGH	HIGH	LOW	LOW
Cyclic	LOW	LOW	LOW	AVERAGE
Stride	LOW	HIGH	LOW	LOW
Temporal	HIGH	LOW	LOW	LOW
Spatial	LOW	HIGH	LOW	LOW
Uniform	LOW	LOW	LOW	AVERAGE
Exponential	AVERAGE	LOW	HIGH	LOW
Normal	LOW	LOW	HIGH	AVERAGE

3.4. Extracting static metrics from inputs

We enrich the hardware counters’ information with input-related metrics derived from analyzing the matrices. The fundamental operations of SpMV, SpADD and SpGEMM concern operating on elements in a row-wise fashion (Algorithms 1 to 3), which inherently leads to high branch misprediction [104, 105] stemming from the fluctuation in the number of nonzero elements in the row. In this setting, Branch Entropy well encapsulates this feature and has been shown to correlate positively with branch miss rate [106]. Equation (1) shows the formula used for computing branch entropy:

$$E = - \sum_{i=1}^N p(S_i) \log p(S_i) \quad (1)$$

$$E_{max} = - \sum_{i=1}^N \frac{1}{N} \log \frac{1}{N} = - \log \frac{1}{N} \quad (2)$$

Where S_i represents the length of a given branch (row size) and $p(S_i)$ the probability of encountering a loop of that size. Branch entropy is then normalized by E_{max} to obtain a value between 0 (no entropy, maximum prediction accuracy) and 1 (maximum entropy, branch outcomes are not predictable).

Secondly, we categorize matrices with respect to the behavior they have on caches. For this, we determine their temporal and spatial locality. A program or input has high temporal locality if, when a particular address is accessed, it is likely that it will be accessed again in the near future. On the other hand, a program or input has high spatial locality if, when a particular address is accessed, addresses that are physically close in memory are likely to be accessed as well. Metrics that appropriately describe temporal and spatial locality are extremely complex to derive from the exploration of just inputs, as they heavily depend on the algorithm to which the inputs are applied. Upon examining the SpMV and SpGEMM algorithms (Section 2) it can be noticed that, from a macroscopic perspective, they exhibit similar scan-and-lookup behavior, where elements on the left-hand side of the operation are streamed (scan) and used to index the right-hand side element (lookup). The left-hand side element does, by definition,

exhibit optimal spatial locality and limited temporal locality, therefore, without loss of generality, we can focus on the locality pattern of just the right-hand side by extracting the list of indices being accessed. A well know instrument to determine the temporal locality of a set of addresses is the Reuse Distance [107], which has been shown to correlate positively to cache misses [108, 109]. Reuse distance is a metric that measures the number of unique memory addresses between two consecutive accesses to the same memory location. If an index is associated with a small reuse distance, the row accessed in the first memory access is likely to still be in the cache when the second memory access occurs. Conversely, the larger the reuse distance value for a given index, the higher the likelihood of the element being served from memory instead of caches, thus increasing the access time. We determine spatial locality by employing the Index Distance, as defined by Fox et al. [110]. This method involves measuring the difference in index numbers between elements that are accessed subsequently by the algorithm. Lower values of average index distance imply that elements accessed subsequently are more likely to belong to the same cache line or to be prefetched together, whereas high values indicate a pattern that is more erratic and less cache/prefetcher friendly. Reuse and index distances are then transformed to log-affinities (Equation (3)) to clamp their values between 0 (no affinity) and 1 (maximum affinity) and to dampen the effect of extremal values [110]: accessing elements millions of indices apart has a similar cache behavior than accessing elements that are thousands of indices apart.

$$\text{reuse_affinity} = \frac{1}{\log_{10}(10 + \text{reuse_distance})} \quad (3)$$

$$\text{index_affinity} = \frac{1}{\log_{10}(10 + \text{index_distance})} \quad (4)$$

Multithreading performance is crucial in sparse algorithms. However, to best exploit the parallel capabilities of a CPU the workload needs to be appropriately partitioned. The computation of SpMV, SpADD, and SpGEMM can be trivially parallelized by partitioning the left-hand side matrix row-wise across multiple threads, as shown in Figure 1. The main drawback of this approach is that heavily imbalanced matrices (e.g. scale-free graphs with few big communities) hinder the multithread scalability of the row-wise partition scheme. To encapsulate this property, we present a metric called Thread Imbalance, computed by determining the average deviation (as a ratio) between the number of nonzeros that each core receives using static partitioning and the optimal number of nonzeros per core (Equation (5)).

$$\text{thread_imbalance} = \frac{1}{T} \sum_{i=1}^T \frac{|nnz_{assigned,i} - nnz_{ideal,i}|}{nnz_{ideal,i}} \quad (5)$$

$$nnz_{ideal,i} = \frac{nnz}{T} \quad (6)$$

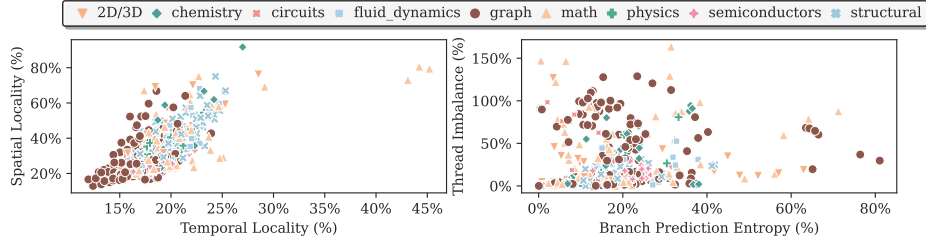


Figure 3: Temporal locality, Spatial locality, Branch entropy and Thread imbalance for our 9 matrix categories.

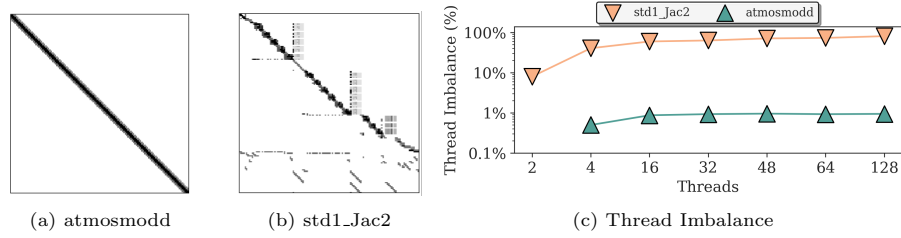


Figure 4: Thread imbalance on two different matrices. (a) and (b) depict the sparse matrices as an adjacency matrix. `atmosmodd` [97] exhibits a more consistent structure than `std1_Jac2` [97] which leads to it having orders of magnitude lower thread imbalance. We omit the value of thread imbalance on two threads for `atmosmodd` since it is 0.

Where T is the number of threads available in a system. For our analysis, we compute thread imbalance for $T \in [2, 4, 16, 32, 48, 64, 128]$. Figure 4 shows how *thread imbalance* reacts to the increase of threads in a balanced (Figure 4a) and in an imbalanced (Figure 4b) matrix. Finally, in spite of several works [111, 112, 22] taking into account the density of a matrix as a relevant metric for characterization, it rarely appeared in the list of most relevant features for a pair of CPU and algorithm. We attribute this to the presence of the other metrics, which are much more fine-grained and are therefore able to be used more efficiently to encapsulate properties of the dataset. The code to compute the aforementioned metrics is publicly available and can be found at <https://gitlab.bsc.es/fsgherzi/spchar-matrix-analyzer>.

Figure 3 displays the metrics for temporal locality, spatial locality, thread imbalance, and branch entropy grouped per matrix category. As expected, temporal and spatial locality are positively correlated ($\rho \approx 0.7$). Moreover, performing the ANOVA [113] statistical test between the matrix categories and the four aforementioned metrics yields p-values below 10^{-10} . Hence we reject the null hypothesis and conclude that there is a statistically relevant correlation between categories and metrics.

3.5. Decision Trees for Extracting Relevant Architectural Insights

Determining what are the most relevant features of an architecture that is interacting with a problem requires knowledge of the problem, the inputs,

and the architecture. However, it is not trivial to determine, for instance, which component of the CPU interacts with which feature of the input or algorithm, as features like the presence of a certain branch predictor could affect, with similar impact, throughput, cycles spent stalling, vector unit utilization and many other factors. Conversely, those three axes cannot be analyzed by themselves in a vacuum: consider the case of a sufficiently small matrix that, in SpMV, has highly random accesses on the dense vector. Architectures that are able to fit the dense vector into cache entirely would yield much higher throughput than architectures that cannot. In SpADD, on the other hand, big or deeper caches are less impactful as the algorithm itself presents a much more regular access pattern to memory, compared to SpMV or SpGEMM.

To extract the most relevant features of an architecture executing a certain algorithm on a given input we employ Tree-Based models [114, 115, 116, 117]: Machine Learning algorithms that work by recursively partitioning the data set into smaller subsets based on the values of different features. In the context of regression (i.e., the objective is to infer a numerical variable), the algorithms select the feature that best separates the data into subsets with different characteristics, choosing the splitting attribute that minimizes the variance of the target variable. This process is repeated for each subset until the data can no longer be meaningfully partitioned. By the end of the process, the algorithm has built a tree-like structure with branches that correspond to different decisions based on the values of different features.

Within the family of tree-based models, there are various options available, with the typical trade-off being between interpretability and performance. In this setting, we employ decision trees, as interpretability is crucial in determining what are the most important features of an architecture. While more sophisticated tree-based models such as Random Forest [114], AdaBoost [115], and Gradient Boosting Trees [116] might yield better performance, they are less interpretable by construction since they build collections of simpler trees and give them more importance the better they are able to predict a certain outcome. Consequently, the individual splitting attributes are not exposed, making it challenging to extract their most relevant features.

Within the scope of hardware architecture, decision trees can be used to analyze the performance of different architectures and identify the features that have the greatest impact on performance [118]. This information can then be used to guide the design of new hardware architectures [117] and optimize them for specific applications [119].

We train our decision tree regressors over a slice of the whole dataset concerning a single algorithm (either SpMV, SpADD or SpGEMM) and a single CPU (either A64FX, Kunpeng 920 or Graviton 3). In this form, the dataset contains a row for each matrix and a column for each value of PMU counters obtained by profiling the given algorithm, as well as the static metrics value associated with it. From this, we remove the PMU counter values that have been used to compute target metrics, which, in the case of Giga Floating Point Operations Per Second (GFLOPS), are ASE_SPEC, VFP_SPEC and execution time. By setting GFLOPS as the target variable, we obtain the splitting attributes

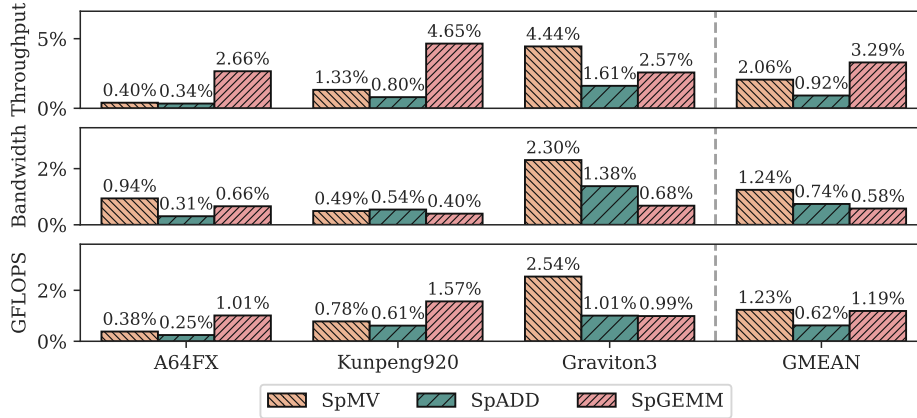


Figure 5: Mean Absolute Percentage Error (MAPE) of 10-fold cross-validation applied to each CPU.

of the decision tree which, in turn, suggest a combination of architectural and most impactful input features. We then confirm the relevance of such attributes by comparing architectures: if an attribute is present among all of them it has a high likelihood of being a characteristic of the algorithm and conversely, if it is not, there exist architectural differences that justify a certain architecture not having a specific bottleneck.

4. Experimental evaluation

In this section, we present the evaluation of our methodology across the three Arm CPUs and the matrix dataset. We first begin by assessing the capability of the decision tree models to encapsulate the properties of the dataset properly. We then move to an evaluation of the synthetic matrices to show how frontend and backend stalls relate to algorithms, inputs and ultimately architectural choices within the CPUs. Finally, we present the analysis of the SpMV, SpADD, and SpGEMM algorithms over the 600 real world matrices and propose key architectural and software improvements that can help overcome the bottlenecks characterizing these algorithms.

4.1. Evaluating Characterization via Decision Trees

Before extracting relevant features from the decision trees, we need to confirm that our models are able to represent our dataset. To this end, we test the performance of our models through K -fold crossvalidation. K -fold crossvalidation works by partitioning the dataset into K slices, training the model on $K - 1$ slices and testing on the leftover slice. This operation is then repeated K times for all resulting permutations of training and testing splits. As target features for prediction, we choose GFLOPS, bandwidth, and throughput, expressed in terms of the number of iterations of the innermost loops for SpMV, SpADD and

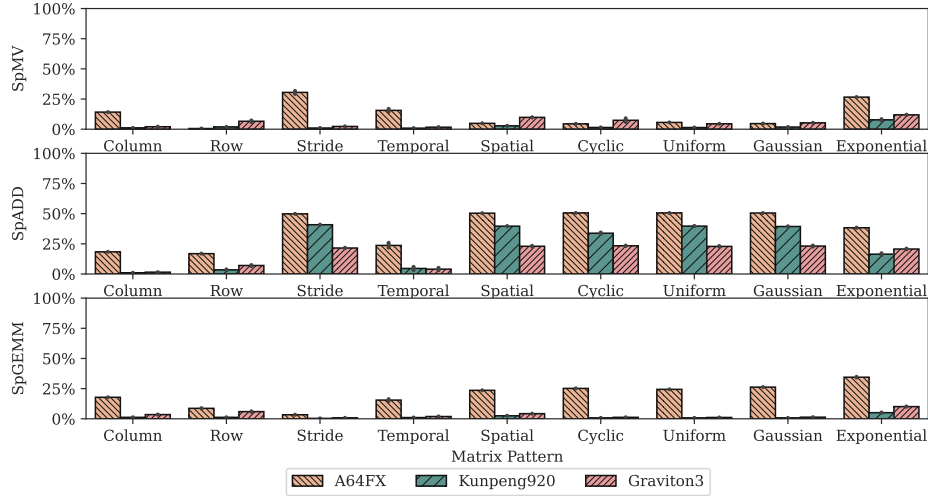


Figure 6: Percentage of Frontend Stalls over all cycles per algorithm and matrix pattern. Heavily branching codes like SpADD stall primarily in the frontend as a result of frequent bad speculation on *data dependent* branches.

SpGEMM. As outlined in Section 3.5, we remove the PMU counters that have been used to compute the target metrics from the dataset before training since this would make it trivial for the algorithm to predict the output perfectly. We use the Mean Absolute Percentage Error (MAPE) to estimate the goodness of our models, which presents a concise way to determine the deviations between predicted and actual values for regressions. In our testing, we opt for $K = 10$, i.e., performing the training and inference stages ten times over ten different partitions, as this value of K is widely used in the literature [120, 121, 122, 123].

Figure 5 displays the average MAPE of the 10-fold crossvalidation per each target metric and each CPU. Our models achieve low percentage error in predicting expected throughput, bandwidth, and GFLOPS for any combination of CPU and algorithm: on average, the MAPE is below 4% indicating that the combination of our choice of performance counters and matrix metrics can accurately predict the target variables. Moreover, the median difference between the predicted and actual value is always below 0.001 (i.e., 0.1%) and coefficient of determination R^2 is always above 0.8 indicating that our models are able to encapsulate the variance of the target features appropriately. We observe that we are able to predict the performance of A64FX and Kunpeng 920 better than Graviton 3, which is due to the fact that both Fujitsu and Huawei provide additional uncore counters in their optimization guide. At the time of writing this document, AWS does not provide documentation containing such PMCs, therefore limiting our models to the counters provided by Arm.

4.2. Evaluating Synthetic Matrices

We proceed with our analysis by showing how our synthetic matrices outline specific bottlenecks of A64FX, Kunpeng 920, and Graviton 3. Figure 6 displays the percentage of cycles stalled in the frontend across our synthetic matrices. A CPU experiences frontend stalls (i.e., instruction fetch and decode) when it cannot feed the execution units with new micro operations, which is commonly associated to instruction cache misses and bad speculation due to branch mispredictions. In our specific use case, kernels like SpMV, SpADD, and SpGEMM are characterized by a limited amount of instructions to be executed at each loop iteration with no variations *across loops*. On the other hand, as outlined in Section 2.1, the kernels in question have branches whose outcome depends on indirectly fetched values. We can therefore consider minimal the impact of instruction cache misses and attribute frontend stalls primarily to pipeline flushes resulting from bad speculation. On matrices that exhibit a more regular structure (Column, Row, Stride, Temporal), frontend stalls are low across the board, as a result of the more predictable row patterns. The Spatial and Cyclic matrices, albeit having a predictable structure in terms of memory accesses, do not have fixed row lengths and, as a result, exhibit similar patterns to the random matrices generated following a particular distribution. SpADD displays consistently high frontend stalls across all platforms and synthetic matrices, as expected from its highly branching code. SpADD is comprised of two nested loops (Algorithm 3), of which the inner depends on the length of the row of the two matrices. As a result, for each row, elements belonging to the rows of the two matrices are either summed (if their indices coincide) or copied into their appropriate slot (if the indices do not coincide). As this decision is data-dependent, it results in frequent bad speculations. Regarding the difference in behavior between CPUs, it can be noted that A64FX has consistently higher frontend stalls, thus indicating that, in this platform, the cost of pipeline flushes resulting from bad speculation is much higher than in the competing platforms.

Figure 7 displays the percentage of cycles stalled in the backend for our synthetic matrices. The backend of the pipeline (i.e., instruction execution and memory operations) stalls when it needs to wait for the execution of arithmetic, vector, or memory instructions, which are particularly lengthy and therefore fill MSHRs, execution units and reorder buffer structures. Sparse codes have generally low operational intensity (i.e., their ratio of memory accesses per arithmetic operation is high), therefore the majority of backend stalls can be attributed to long-latency memory operations, dictated by the latency of the memory subsystem and the number of MSHRs. This is further confirmed by the fact that codes that frequently gather data from indirect accesses (i.e., SpMV and SpGEMM) stall heavily in the backend unless the pattern exhibits sufficient locality. As expected, SpMV is more sensitive to the matrix structure. Upon examining the code (Algorithm 1), it is clear that for each output element, multiple indirect memory accesses have to be performed. This behavior quickly fills the MSHRs, unless the inputs expose high locality while referencing the dense vector. For instance, Column leads to repeated accesses to the same element of the dense

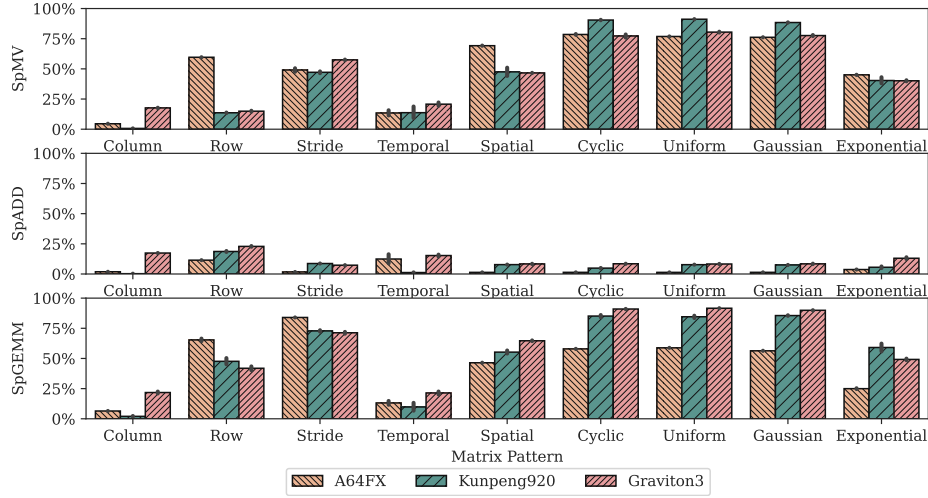


Figure 7: Percentage of Backend Stalls over all cycles per algorithm and matrix pattern. Memory heavy codes like SpMV and SpGEMM incur in high backend stalls as a consequence of poor data locality and limited size of the MSRs.

vector, Row leads to a streaming access pattern on the dense vector, and Temporal also streams the dense vector but in bursts. SpGEMM is similarly affected by this, as it shares the *scan-and-lookup* behavior of SpMV. In contrast to SpMV however, the algorithm exhibits more *intrinsic* locality as rows of both matrices need to be used to compute a single element. As a result, the magnitude of the amount of backend stalls is less dependent on the matrix structure and more dependent on the fact that CPUs need to bring to caches entire rows/columns to compute single elements, which puts a lot of strain on the memory subsystem and trashes the caches. In contrast, SpADD does not exhibit a high amount of backend stalls, due to the fact that both the right-hand and the left-hand side matrices are streamed, resulting in a linear access pattern that exhibits optimal spatial locality.

4.3. Extracting relevant features from decision trees

As outlined in Section 3.5, decision trees work by recursively partitioning the dataset based on the attribute value that minimizes the variance of the target feature. In this context, the amount by which the variance of the target is lowered is referred to as *Gini Importance*. The byproduct of this is that attributes that display stronger relations with the target metric are chosen to be higher in the *tree hierarchy*, whereas less related features appear lower and are given less importance. As a consequence, we can infer an ordering by retrieving the *Gini Importance* of a given attribute, which, in turn, describes the relevance of a feature in predicting the target. For visualization purposes, this relation is displayed in Figures 8, 11 and 14 by assigning to the rectangle containing hardware or input characteristics an area that is proportional to the importance

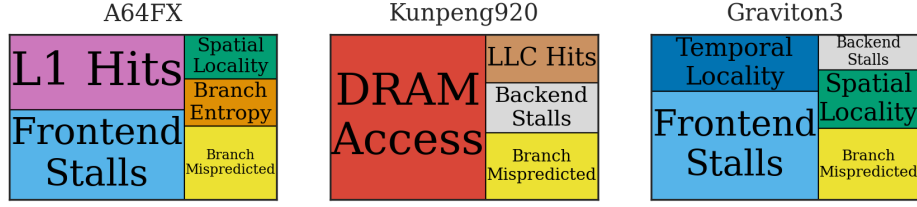


Figure 8: Most relevant input and hardware features for SpMV. SpMV is heavily dependent on the locality of the inputs and the amount of non-zeros per row, which determines the length of the inner loop.

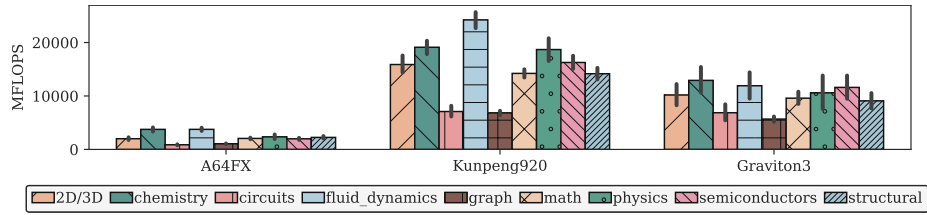


Figure 9: Performance of SpMV per CPU and matrix category. The high number of memory channels of Kunpeng 920, combined with the low latency of DDR4 consistently contributes to higher performance.

of the feature in the induced decision tree. As we use our models for feature extraction and not for inference, we train our models on the entire dataset with the prediction target being GFLOPS.

4.3.1. SpMV

Figure 8 displays the most relevant input and hardware features for each CPU. From this, we draw three findings.

Firstly, in accordance with the state of the art in performance characterization for SpMV [14], we determine that it is primarily bottlenecked by the latency of the memory system. As a result of the indirect access (Algorithm 1), memory accesses are generally not prefetchable which makes the performance of SpMV to be highly reliant on the structure of the matrix (Spatial and Temporal locality attributes). In accordance with this, the better the latency-under-load a system has, the better the performance. To this end, Figure 9 shows the performance in terms of MFLOPS for the three platforms, across matrix categories. Kunpeng 920 yields the best performance across the board, due to the lower memory latency of DDR4 [124], compared to HBM2 in A64FX and DDR5 Graviton 3 and the increased number of memory channels.

Secondly, we observe that frequent bad speculation has a high impact on performance and, on the three platforms we are examining, A64FX and Graviton 3 are the most affected. We investigate this further by examining the percentage of cycles stalled in the frontend and backend for each platform (Figure 10). For Graviton 3 and A64FX, more matrices incur in higher frontend stalls when computing SpMV compared to Kunpeng 920. From this, we determine that,

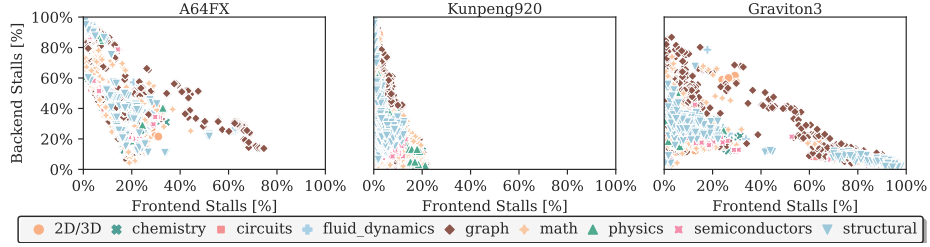


Figure 10: Percentage of cycles spent stalling in the frontend vs backend over all cycles for SpMV. Most of the stalls of Kunpeng 920 are skewed towards the backend, whereas for A64FX and Graviton 3 it leans more towards the frontend.

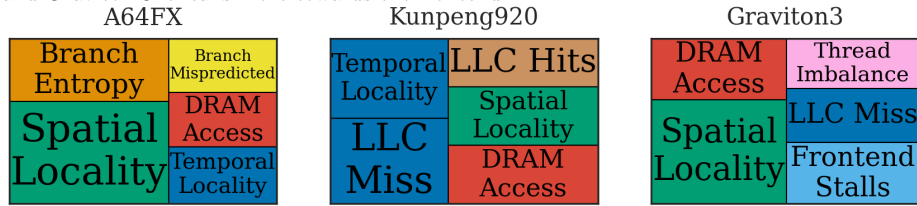


Figure 11: Most relevant model features for SpGEMM: SpGEMM greatly depends on the locality of the input, as a consequence of the frequent cache evictions that the algorithm inherently performs.

while there are architectural features that could help lower the time stalling in the backend (wider MSHR, lower memory latency), reducing frontend stalls from an architectural perspective is much trickier, as a more sophisticated branch predictor would still fail in predicting the outcome of branches when the decision is purely data driven. To overcome this issue, software designers can employ data structures that minimize the likelihood of branch mispredictions [125] to occur and unrolling techniques [30] to enable more efficient vectorization.

Thirdly, we determine that increasing the size of the private core caches and increasing the size of the MSHR can help overcome the dependency of performance from the inputs' locality pattern. Categories that generally exhibit good locality pattern (e.g., structural, semiconductors) see a decrease in the percentage of backend stalls on architectures with bigger caches (Graviton 3, Kunpeng 920). In contrast, randomly structured matrices would benefit from the higher memory level parallelism enabled by wider MSHRs.

4.3.2. SpGEMM

Figure 11 displays the most relevant model features for SpGEMM. From this, we draw two findings. Firstly, in spite of having a similar *scan-and-lookup* memory access pattern as SpMV, the behavior from the cache perspective is much different, as SpGEMM operates on entire rows and columns to produce an individual value of the output matrix.

As a result, caches have a higher likelihood of being polluted by values that are rarely reused after first touch, thus making evictions more frequent. Systems with shallower cache hierarchies such as A64FX are more affected by

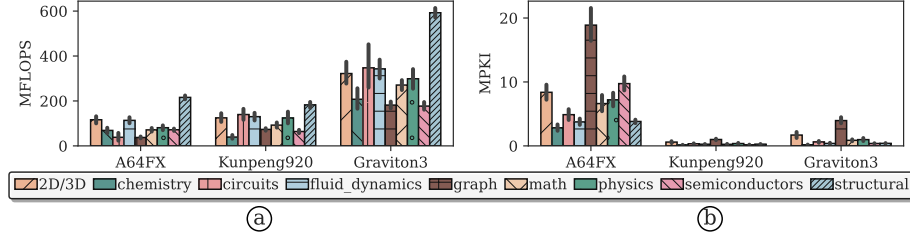


Figure 12: (a) Performance of SpGEMM per CPU and matrix category. Graviton 3 achieves better performances thanks to the combination of bigger caches and wider MSHRs to both exploit the locality of the matrices and having multiple memory requests in flight when needed. (b) Misses Per Kilo Instruction (MPKI) for SpGEMM. Lower cache size and shallower cache hierarchy leads to A64FX having an order of magnitude more MPKI compared to Graviton 3 and Kunpeng 920.

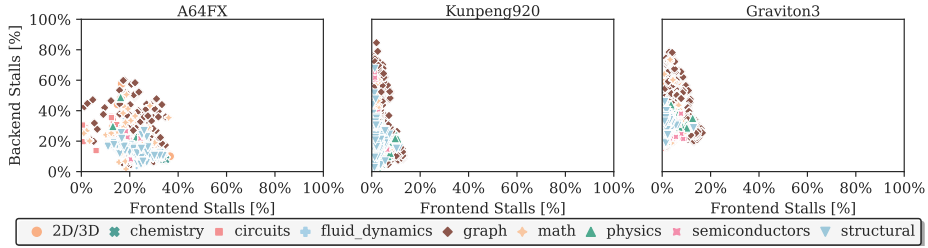


Figure 13: Percentage of cycles spent stalling in the frontend vs backend over all cycles for SpGEMM. Differently from SpMV, CPUs executing SpGEMM stall more frequently waiting for the memory system as a result of inherently poor reuse patterns of the algorithm.

this behavior, as shown in Figure 12 (b), having an order of magnitude more MPKI. Moreover, this puts a heavier strain on the memory system (Figure 13) as new values need to be fed continuously to keep the ALUs active, which results in systems with either lower memory access latency (Kunpeng 920) or bigger MSHRs (Graviton 3) to achieve better performance, as shown in Figure 12 (a).

Secondly, matrix domain has an impact on the performance of SpGEMM. This is not only a byproduct of being sensitive to the locality of the inputs, but also stems from the fact that different matrix categories have different distributions of number of nonzeros across rows. Albeit not as branch-heavy as SpMV, a branch misprediction in SpGEMM still incurs in a high penalty as a result of having to discard the result of plenty of memory instructions when a misprediction occurs.

4.3.3. SpADD

Figure 14 shows the most relevant hardware and input features for each CPU. From this, we draw three findings. Firstly, performance in SpADD is heavily dependent on the pipeline flush overhead that results from a branch misprediction, which is in line with our findings shown in Section 4.2 for the synthetic matrices. As detailed in Section 2.1.4, this kernel stresses the branch

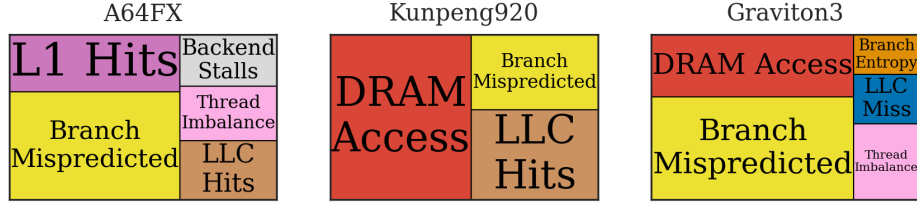


Figure 14: Most relevant model features for SpADD: Non predictable branches are frequent in SpADD, which translates to it being a relevant feature for our models.

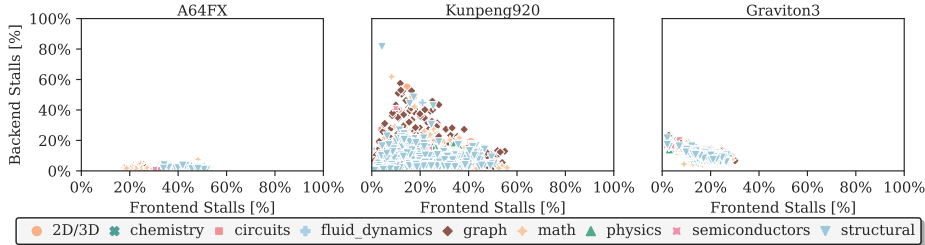


Figure 15: Percentage of cycles spent stalling in the frontend vs backend over all cycles for SpADD. High memory bandwidth and advanced prefetchers limit the time spent stalling in the backend, therefore leaning more towards stalling for branch mispredictions.

predictors heavily due to the continuous *sum-or-merge* operation that occurs for each row. This is only further stressed by the fact that even matrices that have similar structures will incur in this, if the nonzeros in each row are not found in similar positions.

Secondly, stemming from the fact that memory accesses of SpADD are easily prefetchable, platforms with more aggressive prefetchers and higher memory bandwidth achieve better performance. This is confirmed by Figure 15 and Figure 16, where A64FX and Graviton 3 are able to pull up better overall performance compared to Kunpeng 920, as a result of better prefetcher behaviors and higher memory bandwidth.

Thirdly, SpADD is less dependent on the matrix category than SpMV and SpGEMM. The memory accesses performed by this kernel are contiguous, as the matrices are streamed linearly from main memory. As a result, the in-row locality, outlined by the attributes LLC Hits/Miss, is more relevant than the overall locality that would stem from a specific matrix category.

4.4. Optimizing software and hardware architectures for sparse computation

Having discussed what are the most relevant architectures and input features for CPUs performing sparse computation, we now propose suggestions to hardware and software architects to implement efficient architectures and algorithms for sparse computation.

SpMV. If the inputs exhibit low locality, the main performance benefits can be obtained by increasing the capability of the architecture to have multiple outstanding memory operations. This can be performed in two orthogonal ways,

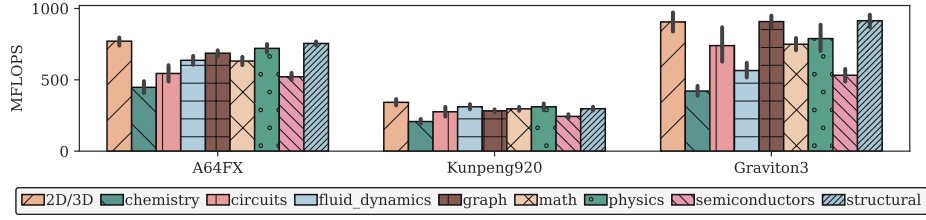


Figure 16: Performance of SpADD per CPU and matrix category. Higher memory bandwidth (A64FX) or better prefetchers (Graviton 3) contributes to higher performance.

by increasing the size of the MSHRs per core and increasing the size of the Reorder Buffer (ROB) or by reducing the *load-to-use* latency. As caches have a low impact in this scenario, using memory technologies and architectures with low latency will prove to be beneficial. Moreover, as the input matrix is streamed and accesses have optimal temporal locality, performance benefits in traditional architectures could be obtained by pairing a high bandwidth memory for streaming and a low latency memory for random accesses in a heterogeneous memory configuration. In turn, this will additionally help reduce the pressure on the memory controllers, as streaming accesses will be relegated to an interface that has, by design, more memory channels. Based on this, Processing In Memory (PIM), Field Programmable Gate Arrays (FPGAs), and decoupled access-execute architectures [126] could be efficiently employed for this kernel. The higher the locality of the input, the lower the impact of the memory subsystem. As a result, the overhead of branch misprediction becomes more relevant. Branch mispredictions stem from the fact that the number of nonzeros in a row of a sparse matrix have high variance. Hence, to overcome this limitation, software architects can employ data representation formats that uniform matrices' rows in fixed size chunks, therefore making branches have a fixed length and rendering them more predictable (ELL and variants [127, 128, 14]).

SpGEMM. Similarly to SpMV, SpGEMM exhibits a *scan-and-lookup* behaviour. As a result, the recommendations that apply to SpMV also apply to SpGEMM. Additionally, the performance of SpGEMM is greatly dependent on the locality of the inputs. Low locality implies continuous cache evictions resulting from fetching entire rows/columns of the matrices to perform the computation of single output values. Therefore, the major performance improvements would be obtained by using large caches or forcing more input locality via matrix reordering [129], and block-based partitioning mechanisms.

SpADD. SpADD is much less dependent on the matrix structure, having both input matrices being streamed to perform the computation. As a result, it benefits greatly from prefetching and having a high bandwidth memory subsystem. The heavy branching behavior can be overcome by using data structures that regularize the branching pattern. In this regard, formats that would benefit SpADD the most are 2D block-based [14, 130, 131], combining coalesced memory accesses at the row-level with predictable branching behavior.

4.5. Summary and applicability of the SpChar methodology

In this section, we have introduced a new methodology apt to determine the features that are most impactful for sparse computation. This is achieved by extracting insights from static input metrics and PMU counters. We have then analyzed these insights to provide suggestions to software and hardware architects seeking to optimize sparse computation.

The next step would be to prove that the optimizations we propose are effective and to provide quantitative data on the potential improvements. To this end, Section 5 uses the SpMV kernel as a use case to explore the optimization proposed, and relates them to matrices that display the specific structures we have outlined to be problematic for sparse computation.

As stated in Section 4.4, key factors influencing SpMV performance are the memory subsystem’s latency for indirect access, its bandwidth for streaming accesses, and the efficiency of the frontend in managing the cost of incorrect speculation. Therefore, architectural enhancements for SpMV should focus on enabling the architecture to feed data to the core with reduced latency and minimizing the impact of frontend stalls. These optimizations can be translated to increasing the size of MSHRs and ROB, as well as employing prefetchers. Additionally, memory interfaces should be selected based on the access pattern they primarily service. We explore these parameters in Section 5.

5. Optimizing SpMV through SpChar: the Characterization Loop

To complete the characterization loop that SpChar provides, we now implement the suggestions we have made in Section 4.4. To this end, we analyze a common use case of optimizing an architecture for the execution of the SpMV kernel.

Table 4: Summary of the features of the simulated CPU

Architecture	ARM v8.2-a
Cores	16 Out Of Order Cores at 2.4GHz
Vector units	$2 \times$ 256-bit SVE
L1D, L1I per core	64 kB, 4-way, 2 cycle data access
Private L2 per core	1 MB, 8-way, 4 cycle data access
Shared LLC	$16 \times$ 1 MB, 16-way, 10 cycle data access
Network-on-chip	8×8 2D mesh with AMBA 5 CHI, 1-cycle route and link latency
Memory technology	DDR5, HBM2e
Memory channels	4, 8
NUMA Nodes	2
Peak bandwidth	452.8 GB/s
Operating System	Ubuntu 22.04
Compiler	g++ 11.3.1

Table 5: Summary of the explored parameters. Values in bold indicate the default.

L1D MSHRs	8 , 16, 32
L1D Prefetcher	None , Stride-degree 2
L2 MSHRs	16 , 32, 64
L2 Prefetcher	None , Best Offset [132]
LLC MSHRs	32 , 64, 128
ROB size	224 , 554
Addr. mapping for Memory Device	RoCoRaBaCh , RoRaBaChCo
Memory Row Policy	open , close
Vectorization	Compiler , SVE Intrinsics
Sparse Matrix Location	DDR5 , HBM2e
Dense Vector Location	DDR5 , HBM2e

Table 6: Summary of the presented configurations.

ID	Explored Parameters
C1	Defaults (bold parameters in Table 5)
C2	C1 + L1D, L2 prefetchers
C3	C2 + 32, 64, 128 MSHRs for L1D, L2, LLC respectively
C4	C3 + 554 ROB entries
C5	C4 + Dense Vector in DDR5 & Sparse Matrix in HBM2e DDR5 uses closed row policy and RoCoRaBaCh Addr. mapping. HBM2e uses open row policy and RoRaBaChCo Addr. mapping.

We use the gem5 simulator [18] to simulate a 16-core Arm SoC, based on the Neoverse N1 architecture. The Network On Chip (NOC) is designed to support two NUMA nodes. Each NUMA node is associated with a specific type of memory technology – one with four channels of DDR5 memory and the other with 8 channels of HBM2e. CPU features are displayed in Table 4. Starting from this configuration, we consider the performance bottlenecks that affect it and incrementally alleviate them by changing a single architectural feature (Table 5) at a time, thus allowing us to determine the individual contribution of each feature to the performance increase. We repeat this loop of choosing an architectural feature, applying it, benchmarking, and analyzing the impact on performance until we exhaust the exploration space. Due to space constraints, we present five notable configurations, outlined in Table 6.

The first architectural optimization we test is the inclusion of private cache prefetchers (**C2**), which aid in streaming the sparse matrix. Configuration **C3** tackles the issue of tolerating cache misses by increasing the MSHRs’ size, thus easing the burden of random accesses to the dense vector. Configuration **C4** builds upon **C3** by increasing the size of the reorder buffer, hence increasing the number of in-flight memory requests that the CPUs can have. Finally, **C5**

tackles the issue of having streaming-like accesses on the sparse matrix and random accesses on the dense vector. To this end, we place the data structures that are accessed in a streaming fashion in HBM2e on NUMA Node 1 and the ones that are accessed randomly on DDR5 on NUMA Node 0 using the `numa_alloc_onnode` function from `libnuma`. Additionally, we tweak the address mapping and row policy of such interfaces to optimize the accesses they ought to serve. In this setting, HBM2e operates under the Open Row policy (i.e., keep the row buffer open after access) with the RoRaBaChCo (row, rank, bank, channel, column) address mapping. This configuration capitalizes on linear accesses as contiguous addresses are more likely to hit a bank that is already precharged. Conversely, DDR5 operates under Closed Row policy (i.e, banks are precharged after every access) and the RoCoRaBaCh (row, column, rank, bank, channel) address mapping. Random accesses are not expected to hit a row buffer that is already open, hence, by closing it after access, bank precharge times are not on the critical path.

Table 7: Matrices used in the evaluation and their characteristics, sorted by number of non-zero entries. The labels LOW, AVERAGE, HIGH refer to the a metric being below the first quartile (Q1), within the first and third quartile (Q1-Q3), and above the third quartile (Q3), respectively.

Name	ID	Rows	NNZ	Temporal Loc.	Spatial Loc.	Row Imbalance	Branch Entropy
std1.Jac2	M1	22K	1.2M	HIGH	HIGH	AVERAGE	AVERAGE
test1	M2	392.9K	13.0M	HIGH	LOW	AVERAGE	AVERAGE
nd12k	M3	36.0K	14.2M	HIGH	HIGH	HIGH	AVERAGE
TSOPF_RS_b2383	M4	38.1K	16.2M	LOW	LOW	HIGH	HIGH
human_gene2	M5	14.3K	18.1M	HIGH	HIGH	HIGH	AVERAGE
Transport	M6	1602.1K	23.5M	LOW	AVERAGE	LOW	LOW
nd24k	M7	72.0K	28.7M	HIGH	HIGH	HIGH	AVERAGE
mawi_201512012345	M8	18571.2K	38.0M	AVERAGE	HIGH	LOW	HIGH
spal.004	M9	10.2K	46.2M	HIGH	AVERAGE	HIGH	LOW

To limit exploration and simulation times, we test our configurations on a subset of 9 matrices from our main real-world dataset. To this end, we choose the top 2 matrices that had the highest (for branch entropy and thread imbalance) or lowest (index and reuse affinity) values of the four static metrics that we have presented in Section 3, plus a small matrix (**M1**) to outline the effect of being able to cache the data structures involved in the computation entirely. The selected matrices are detailed in Table 7.

Figure 17 shows the speedup of each configuration normalized to **C1**. From this, we draw three conclusions.

Firstly, adding private cache prefetchers (**C2**) reduces the execution time by an average 31%. While the accesses on the dense vector are generally not predictable, the 80% of the data involved in the computation (i.e., output, nonzero, row pointer, column index vectors) is accessed linearly, resulting in prefetchers being able to gather data from memory beforehand effectively. On the other hand, this category of prefetchers fail in proactively retrieving the next datum from the dense vector, as they are unable to infer access patterns in indirect, random accesses. While prefetchers like Indirect Memory Prefetcher (IMP) [133] might yield better performance, they would only directly benefit

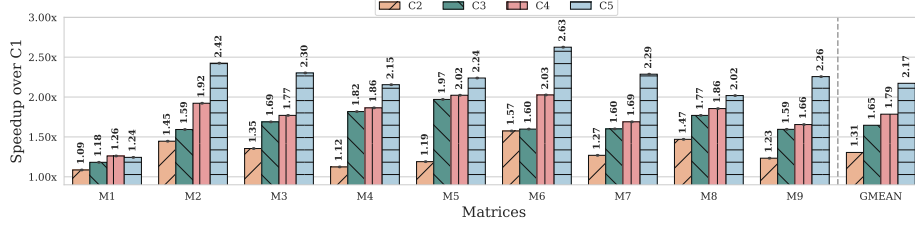


Figure 17: Speedup with respect to default configuration (**C1**). Having dedicated memory interfaces for streaming and random accesses greatly improves execution times (**C3**).

kernels with this kind of access pattern and not improve applications that use this kernel along with others [2, 1, 50].

Secondly, enhancing the capabilities of having more memory requests in-flight (**C4**) improves performance by an average 79% over the baseline. We further examine this in Figure 19, where we present the roofline for our configurations across all inputs. SpMV has low arithmetic intensity, consequence of relying on multiple memory requests to compute a single output value (Algorithm 1). Hence, increasing the MSHRs’ size empowers the CPU to handle more misses without stalling, and increasing the ROB size allows for more independent load instructions to be queued. While these configurations are able to achieve only up 30% of peak bandwidth utilization, increasing the capability of having more memory requests in-flight essentially doubles the bandwidth utilized w.r.t. **C1**.

Thirdly, having an interface optimized for bandwidth and one for latency in configuration **C5** improves performance by an additional 40% over configuration **C4** and $2.17\times$ over the baseline. This is due to (i) better exploit the increased number of channels of HBM2e, which is able to meet the high bandwidth requirements of streaming the sparse matrix without having to handle random accesses, (ii) the Open Row policy of HBM2e which prevents DRAM row buffers to be closed upon access, thus capitalizing on the fact that row buffer misses occur sporadically in streaming accesses, (iii) the Closed Row policy of DDR5, which immediately closes the row buffer upon access and thus capitalizes on the bank precharge times not being on the critical path.

Finally, we observe that the size and locality of the input play a major role in how the proposed optimized architectures improve performance. First, if all the computational elements are able to fit in cache (**M1**), our optimizations yield limited benefits, which is a given of the fact that we mainly focus on optimizing for memory latency. Second, we observe that increasing the ROB size yields noticeable improvements in matrices with low Temporal Locality (**M2**, **M6**) while providing marginal speedups in higher locality inputs. For those inputs, increasing the MSHRs’ size already yields a sufficient increase of in-flight memory requests, which are able to be filled before the MSHRs’ are exhausted.

Figure 18 shows the average load-to-use-latency for each architecture and

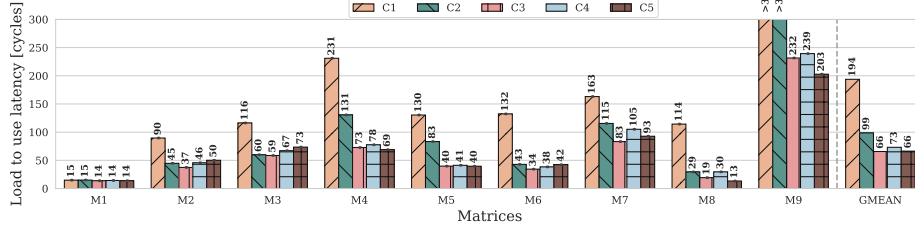


Figure 18: Load to use latency for our five configurations.

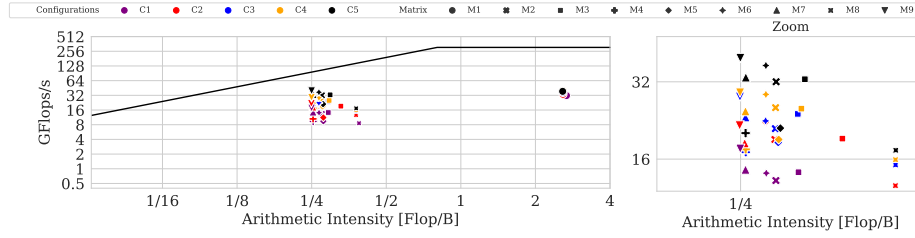


Figure 19: Roofline of our five configurations: our optimized configurations consistently yield an increase in throughput, up to $1.8\times$ on average.

input matrix. We observe that configuration **C5** yields an average reduction of $\approx 65\%$ in load-to-use latency. Moreover, we observe that such reduction is correlated with the matrix density, impacting more favorably sparser matrices (**M6**, **M7**, **M8**, **M9**). While all of our optimizations are effective in this scenario, adding private caches’ prefetchers and increasing the MSHRs’ size are the optimizations that yield the most improvement, that is, 49% improvement using **C2** and an additional 33% improvement using **C3**.

Overall, as outlined in Section 4.4, increasing the number of in-flight memory requests and reducing the pressure on the memory controllers are effective optimizations for SpMV. Furthermore, our analysis shows that the most relevant improvements are obtained by optimizing memory interfaces for the type of access they ought to serve. In this setting, we are able to best exploit the bandwidth of HBM2e by performing streaming accesses exclusively on this interface and relinquishing all random accesses on an interface optimized for latency (DDR5).

6. Related Work

To our knowledge, this is the first work that employs tree-based models to identify the most relevant hardware and input characteristics, starting from hardware and input-related metrics gathered from PMCs and matrices. There have been numerous characterization studies of Sparse Kernels in the literature, we now briefly discuss related prior work.

There is a large body of research on comparisons across existing machines and instruction set architectures. Mantovani et al. [134] evaluate thread and node scalability on the Marenostrum 4 Supercomputer and Thunder X2 equipped systems. They compare performance and energy consumption, discuss microarchitectural choices (e.g., size of vector units or cache hierarchy) and conclude that Arm architectures are mature enough to debut in next-generation HPC systems. Armejach et al. [135] evaluate various heterogeneous HPC architectures employing different combinations of in-order and out-of-order cores as well as LLC sizes per core and conclude that scaling LLCs yields diminishing returns performance-wise, while having a noticeable impact on area and power utilization. Poenaru et al. [136] compare ARM (AWS Graviton2, Cavium TX2, Ampere Altra) and X86_64 (Intel Cascade Lake, AMD Rome) platforms using both mini-applications and full-scale codes with different compilers ([137, 138] for TX2). Oliveira et al. [139] evaluate ARM, PowerPC and X86 platforms for HPC via different metrics (e.g., GFLOPS per Watt, GFLOPS versus memory bandwidth or bytes per FLOP). For the specific case of ARM, they find that theoretical peak performances are much further away from sustained performances with respect to other mainstream platforms.

Others have focused on using specific metrics for characterization. Bean et al. [140] characterize data movement of memory-intensive benchmarks by profiling an Intel Xeon platform with VTune. Then they run those benchmarks on a simulator to explore the impact of microarchitectural choices on the benchmark. Later, they classify the applications by the amount of spatial and temporal locality, and gather insights using MPKI, last to first level cache ratio, and operational intensity. Finally, they divide the problems into 6 classes, whose classification is dependent on how high/low the 3 metrics are. Cabezas et al. [141] extend the roofline model with throughput, latency and cache capacity. They use instrumentation of the code to build a dependency graph, from which they estimate bottlenecks.

Some works looked at the impact of sparse matrix formats. For example, Asgari et al. [142] discuss the performance implications of different sparse matrix formats. They focus on the decompression stage for non-standard formats using 20 matrices and provide a connection from matrix formats to applications. Alappat et al. [23] evaluate SpMV and Lattice quantum chromodynamics domain wall kernels on the A64FX platform comparing different matrix formats (CSR and SELL-C) to show which one is the most suitable. This work provides comprehensive architectural details and performance optimizations for A64FX. Finally, they build a model for single core execution time by taking into account architectural details like memory load time and instruction overlap.

We also find several Sparse kernel acceleration efforts in the literature. Some examples include FPGA-based [143, 144, 145, 146, 53, 147], dedicated hardware accelerators [148, 149, 150, 151, 152, 153, 154, 155, 156, 157, 158, 159], real PIM platforms [14] or exploitation of software/hardware co-design [32, 160, 161]. Finally, Lee et al. [162] find that, with appropriate optimizations, CPUs and GPUs can share similar performance regimes.

Regarding the use of ML to predict performance, Chen et al. [22] evaluate

the scalability of SpMV from 1 to 4 cores, considering multiple matrices (1000+) from different categories. They build an ML model to predict scalability from PMC counters and different matrix metrics. While their approach is similar to ours, they only target scalability prediction in the context of a single CPU architecture and algorithm. Therefore, their feature extraction method is limited in scope and may not apply to different architectures and algorithms.

Therefore, none of these works perform a detailed characterization for a broad number of sparse kernels, inputs, and CPUs. SpChar aims to fill this gap and to give guidance to software and hardware designers in developing solutions optimized for sparse computation.

7. Conclusion

In this work, we present SpChar, a workload characterization methodology for general sparse computation. SpChar is based on tree-based models to identify the most relevant hardware and input characteristics, starting from hardware and input-related metrics gathered from PMCs and matrices. SpChar’s contributions are threefold: (1) it enables the characterization of sparse computation from the perspective of inputs, algorithms and architectures, (2) it determines what are the most impactful features for future architectures to excel in this field by gathering architectural insights, and (3) it creates a new analysis method to establish a characterization loop that could enable hardware and software designers to map the impact of architectural features to algorithmic choices and inputs. Our evaluation, which considers more than 600 matrices and various sparse kernels, determines that the biggest limiting factors for high-performance sparse computation are (1) the latency of the memory system, (2) the pipeline flush overhead due to branch misprediction and (3) the poor reuse of cached elements. We test the SpChar methodology applied to the common use case of optimizing the SpMV kernel obtaining considerable performance improvements, hence SpChar is successfully able to create a characterization loop that enables software and hardware architects to map architectural features to inputs and algorithms, and optimize accordingly.

8. Acknowledgment

This research was supported by: the Spanish Ministry of Science and Innovation (MCIN) through contracts PID2019-107255GB-C21, PID2019-107255GB-C21 (MCIN/AEI/10.13039/501100011033) and the European Processor Initiative (EPI) under grant agreement No. 101036168. M. Siracusa has been partially supported by an FI fellowship (2022FI.B 00969). Finally, A. Armejach is a Serra Hunter Fellow.

References

- [1] A. Parravicini, L. G. Cellamare, M. Siracusa, M. D. Santambrogio, Scaling up HBM efficiency of Top-K SpMV for approximate embedding similarity

- on FPGAs, in: 2021 58th ACM/IEEE Design Automation Conference (DAC), IEEE, 2021, pp. 799–804.
- [2] A. Parravicini, F. Sgherzi, M. D. Santambrogio, A reduced-precision streaming SpMV architecture for Personalized PageRank on FPGA, in: 2021 26th Asia and South Pacific Design Automation Conference (ASP-DAC), IEEE, 2021, pp. 378–383.
 - [3] G. Rakocevic, V. Semenyuk, W.-P. Lee, J. Spencer, J. Browning, I. J. Johnson, V. Arsenijevic, J. Nadj, K. Ghose, M. C. Suciu, et al., Fast and accurate genomic analyses using genome graphs, *Nature genetics* 51 (2) (2019) 354–362.
 - [4] M. Baskaran, B. Meister, N. Vasilache, R. Lethin, Efficient and scalable computations with sparse tensors, in: 2012 IEEE Conference on High Performance Extreme Computing, IEEE, 2012, pp. 1–6.
 - [5] T. Brown, B. Mann, N. Ryder, M. Subbiah, J. D. Kaplan, P. Dhariwal, A. Neelakantan, P. Shyam, G. Sastry, A. Askell, et al., Language models are few-shot learners, *Advances in neural information processing systems* 33 (2020) 1877–1901.
 - [6] R. Rombach, A. Blattmann, D. Lorenz, P. Esser, B. Ommer, High-resolution image synthesis with latent diffusion models, in: Proceedings of the IEEE/CVF Conference on Computer Vision and Pattern Recognition, 2022, pp. 10684–10695.
 - [7] O. Sharir, B. Peleg, Y. Shoham, The cost of training nlp models: A concise overview, *arXiv preprint arXiv:2004.08900* (2020).
 - [8] E. Strubell, A. Ganesh, A. McCallum, Energy and policy considerations for deep learning in NLP, *arXiv preprint arXiv:1906.02243* (2019).
 - [9] X. Zhou, W. Zhang, H. Xu, T. Zhang, Effective sparsification of neural networks with global sparsity constraint, in: Proceedings of the IEEE/CVF Conference on Computer Vision and Pattern Recognition, 2021, pp. 3599–3608.
 - [10] H. Peng, D. Gurevin, S. Huang, T. Geng, W. Jiang, O. Khan, C. Ding, Towards sparsification of graph neural networks, in: 2022 IEEE 40th International Conference on Computer Design (ICCD), IEEE, 2022, pp. 272–279.
 - [11] X. Zhou, W. Zhang, Z. Chen, S. Diao, T. Zhang, Efficient neural network training via forward and backward propagation sparsification, *Advances in Neural Information Processing Systems* 34 (2021) 15216–15229.
 - [12] T. Hoefer, D. Alistarh, T. Ben-Nun, N. Dryden, A. Peste, Sparsity in deep learning: Pruning and growth for efficient inference and training in neural networks, *The Journal of Machine Learning Research* 22 (1) (2021) 10882–11005.

- [13] Y. Umuroglu, M. Jahre, Random access schemes for efficient FPGA SpMV acceleration, *Microprocessors and Microsystems* 47 (2016) 321–332.
- [14] C. Giannoula, I. Fernandez, J. G. Luna, N. Koziris, G. Goumas, O. Mutlu, SparseP: Towards Efficient Sparse Matrix Vector Multiplication on Real Processing-In-Memory Architectures, *Proc. ACM Meas. Anal. Comput. Syst.* 6 (1) (Feb. 2022). doi:10.1145/3508041.
URL <https://doi.org/10.1145/3508041>
- [15] S. Byna, Y. Chen, X.-H. Sun, A taxonomy of data prefetching mechanisms, in: *2008 International Symposium on Parallel Architectures, Algorithms, and Networks (i-span 2008)*, IEEE, 2008, pp. 19–24.
- [16] P. Malakar, P. Balaprakash, V. Vishwanath, V. Morozov, K. Kumaran, Benchmarking machine learning methods for performance modeling of scientific applications, in: *2018 IEEE/ACM Performance Modeling, Benchmarking and Simulation of High Performance Computer Systems (PMBS)*, IEEE, 2018, pp. 33–44.
- [17] N. Wu, Y. Xie, A survey of machine learning for computer architecture and systems, *ACM Computing Surveys (CSUR)* 55 (3) (2022) 1–39.
- [18] J. Lowe-Power, A. M. Ahmad, A. Akram, M. Alian, R. Amslinger, M. Andreozzi, A. Armejach, N. Asmussen, B. Beckmann, S. Bharadwaj, et al., The gem5 simulator: Version 20.0+, *arXiv preprint arXiv:2007.03152* (2020).
- [19] I. Wang, P. Chakraborty, Z. Y. Xue, Y. F. Lin, Evaluation of gem5 for performance modeling of ARM Cortex-R based embedded SoCs, *Microprocessors and Microsystems* 93 (2022) 104599.
- [20] I. Nisa, C. Siegel, A. S. Rajam, A. Vishnu, P. Sadayappan, Effective machine learning based format selection and performance modeling for SpMV on GPUs, in: *2018 IEEE International Parallel and Distributed Processing Symposium Workshops (IPDPSW)*, IEEE, 2018, pp. 1056–1065.
- [21] A. Benatia, W. Ji, Y. Wang, F. Shi, Machine learning approach for the predicting performance of SpMV on GPU, in: *2016 IEEE 22nd International Conference on Parallel and Distributed Systems (ICPADS)*, IEEE, 2016, pp. 894–901.
- [22] D. Chen, J. Fang, C. Xu, S. Chen, Z. Wang, Characterizing scalability of sparse matrix-vector multiplications on phyium ft-2000+, *International Journal of Parallel Programming* 48 (1) (2020) 80–97.
- [23] C. Alappat, N. Meyer, J. Laukemann, T. Gruber, G. Hager, G. Wellein, T. Wettig, Execution-Cache-Memory modeling and performance tuning of sparse matrix-vector multiplication and Lattice quantum chromodynamics on A64FX, *Concurrency and Computation: Practice and Experience* 34 (20) (2022) e6512.

- [24] R. Barrett, M. Berry, T. F. Chan, J. Demmel, J. Donato, J. Dongarra, V. Eijkhout, R. Pozo, C. Romine, H. van der Vorst, Templates for the Solution of Linear Systems: Building Blocks for Iterative Methods, Society for Industrial and Applied Mathematics, 1994. [arXiv:https://epubs.siam.org/doi/pdf/10.1137/1.9781611971538](https://epubs.siam.org/doi/pdf/10.1137/1.9781611971538), doi:10.1137/1.9781611971538. URL <https://epubs.siam.org/doi/abs/10.1137/1.9781611971538>
- [25] E. jin Im, K. Yelick, Optimizing Sparse Matrix Computations for Register Reuse in SPARSITY, in: In Proceedings of the International Conference on Computational Science, volume 2073 of LNCS, Springer, pp. 127–136.
- [26] D. Langr, P. Tvrđík, Evaluation Criteria for Sparse Matrix Storage Formats, IEEE Transactions on Parallel and Distributed Systems 27 (2) (2016) 428–440. doi:10.1109/TPDS.2015.2401575.
- [27] F. G. Gustavson, Two Fast Algorithms for Sparse Matrices: Multiplication and Permuted Transposition, ACM Trans. Math. Softw. 4 (3) (1978) 250–269. doi:10.1145/355791.355796. URL <https://doi.org/10.1145/355791.355796>
- [28] S. Williams, L. Oliker, R. Vuduc, J. Shalf, K. Yelick, J. Demmel, Optimization of sparse matrix-vector multiplication on emerging multicore platforms, in: SC '07: Proceedings of the 2007 ACM/IEEE Conference on Supercomputing, 2007, pp. 1–12. doi:10.1145/1362622.1362674.
- [29] S. Beamer, K. Asanović, D. Patterson, The GAP Benchmark Suite (2015). doi:10.48550/ARXIV.1508.03619. URL <https://arxiv.org/abs/1508.03619>
- [30] C. Gómez, F. Mantovani, E. Focht, M. Casas, Efficiently running SpMV on long vector architectures, in: Proceedings of the 26th ACM SIGPLAN Symposium on Principles and Practice of Parallel Programming, 2021, pp. 292–303.
- [31] Y. Yang, J. S. Emer, D. Sanchez, SpZip: Architectural Support for Effective Data Compression In Irregular Applications, in: 2021 ACM/IEEE 48th Annual International Symposium on Computer Architecture (ISCA), 2021, pp. 1069–1082. doi:10.1109/ISCA52012.2021.00087.
- [32] K. Kanellopoulos, N. Vijaykumar, C. Giannoula, R. Azizi, S. Kopula, N. M. Ghiasi, T. Shahroodi, J. G. Luna, O. Mutlu, Smash: Co-designing software compression and hardware-accelerated indexing for efficient sparse matrix operations, in: Proceedings of the 52nd annual IEEE/ACM international symposium on microarchitecture, 2019, pp. 600–614.

- [33] C. Yang, A. Buluç, J. D. Owens, Design principles for sparse matrix multiplication on the gpu, in: Euro-Par 2018: Parallel Processing: 24th International Conference on Parallel and Distributed Computing, Turin, Italy, August 27-31, 2018, Proceedings, Springer, 2018, pp. 672–687.
- [34] S. E. Kurt, S. Raje, A. Sukumaran-Rajam, P. Sadayappan, Sparsity-Aware Tensor Decomposition, in: 2022 IEEE International Parallel and Distributed Processing Symposium (IPDPS), IEEE, 2022, pp. 952–962.
- [35] J. Gao, W. Ji, Z. Tan, Y. Zhao, A Systematic Survey of General Sparse Matrix-Matrix Multiplication (2020). [arXiv:2002.11273](https://arxiv.org/abs/2002.11273).
- [36] M. T. Hussain, G. S. Abhishek, A. Buluç, A. Azad, Parallel Algorithms for Adding a Collection of Sparse Matrices (2021). [doi:10.48550/ARXIV.2112.10223](https://arxiv.org/abs/2112.10223).
URL <https://arxiv.org/abs/2112.10223>
- [37] F. Kjolstad, S. Kamil, S. Chou, D. Lugato, S. Amarasinghe, The Tensor Algebra Compiler, Proc. ACM Program. Lang. 1 (OOPSLA) (Oct. 2017). [doi:10.1145/3133901](https://doi.org/10.1145/3133901).
URL <https://doi.org/10.1145/3133901>
- [38] A. Ng, M. Jordan, Y. Weiss, On spectral clustering: Analysis and an algorithm, Advances in neural information processing systems 14 (2001).
- [39] T. F. Coleman, J. J. Moré, Estimation of sparse Jacobian matrices and graph coloring blems, SIAM journal on Numerical Analysis 20 (1) (1983) 187–209.
- [40] Y. El-Kurdi, D. Giannacopoulos, W. J. Gross, Hardware acceleration for finite-element electromagnetics: Efficient sparse matrix floating-point computations with FPGAs, IEEE Transactions on Magnetics 43 (4) (2007) 1525–1528.
- [41] J. Dongarra, M. A. Heroux, P. Luszczek, Hpcg benchmark: a new metric for ranking high performance computing systems, Knoxville, Tennessee 42 (2015).
- [42] P. Stathis, S. Vassiliadis, S. Cotofana, D-sab: A sparse matrix benchmark suite, in: International Conference on Parallel Computing Technologies, Springer, 2003, pp. 549–554.
- [43] A. Andreev, A. Nasonov, A. Novokshchenov, A. Bochkarev, E. Kharkov, D. Zharikov, S. Kharchenko, A. Yuschenko, Vectorization algorithms of block linear algebra operations using SIMD instructions, Communications in Computer and Information Science 535 (2015) 323–340.
- [44] A. R. Carneiro, M. S. Serpa, P. O. Navaux, Lightweight Deep Learning Applications on AVX-512, in: 2021 IEEE Symposium on Computers and Communications (ISCC), IEEE, 2021, pp. 1–6.

- [45] C. A. Navarro, R. Carrasco, R. J. Barrientos, J. A. Riquelme, R. Vega, GPU tensor cores for fast arithmetic reductions, *IEEE Transactions on Parallel and Distributed Systems* 32 (1) (2020) 72–84.
- [46] A. Haidar, S. Tomov, J. Dongarra, N. J. Higham, Harnessing GPU tensor cores for fast FP16 arithmetic to speed up mixed-precision iterative refinement solvers, in: *SC18: International Conference for High Performance Computing, Networking, Storage and Analysis*, IEEE, 2018, pp. 603–613.
- [47] T. De Matteis, J. de Fine Licht, T. Hoefer, FBLAS: Streaming linear algebra on FPGA, in: *SC20: International Conference for High Performance Computing, Networking, Storage and Analysis*, IEEE, 2020, pp. 1–13.
- [48] K. Kara, D. Alistarh, G. Alonso, O. Mutlu, C. Zhang, FPGA-accelerated dense linear machine learning: A precision-convergence trade-off, in: *2017 IEEE 25th Annual International Symposium on Field-Programmable Custom Computing Machines (FCCM)*, IEEE, 2017, pp. 160–167.
- [49] M. Martineau, P. Atkinson, S. McIntosh-Smith, Benchmarking the nvidia v100 gpu and tensor cores, in: *European Conference on Parallel Processing*, Springer, 2019, pp. 444–455.
- [50] F. Sgherzi, A. Parravicini, M. D. Santambrogio, A Mixed Precision, Multi-GPU Design for Large-scale Top-K Sparse Eigenproblems, in: *2022 IEEE International Symposium on Circuits and Systems (ISCAS)*, 2022, pp. 1259–1263. doi:10.1109/ISCAS48785.2022.9937893.
- [51] A. Benatia, W. Ji, Y. Wang, F. Shi, Sparse matrix partitioning for optimizing SpMV on CPU-GPU heterogeneous platforms, *The International Journal of High Performance Computing Applications* 34 (1) (2020) 66–80.
- [52] A. Elafrou, V. Karakasis, T. Gkountouvas, K. Kourtis, G. Goumas, N. Koziris, SparseX: A library for high-performance sparse matrix-vector multiplication on multicore platforms, *ACM Transactions on Mathematical Software (TOMS)* 44 (3) (2018) 1–32.
- [53] M. Siracusa, E. Del Sozzo, M. Rabozzi, L. Di Tucci, S. Williams, D. Sciuto, M. D. Santambrogio, A Comprehensive Methodology to Optimize FPGA Designs via the Roofline Model, *IEEE Transactions on Computers* 71 (8) (2022) 1903–1915. doi:10.1109/TC.2021.3111761.
- [54] A. Elafrou, G. Goumas, N. Koziris, Performance analysis and optimization of sparse matrix-vector multiplication on intel xeon phi, in: *2017 IEEE International Parallel and Distributed Processing Symposium Workshops (IPDPSW)*, IEEE, 2017, pp. 1389–1398.
- [55] G. Goumas, K. Kourtis, N. Anastopoulos, V. Karakasis, N. Koziris, Understanding the performance of sparse matrix-vector multiplication, in:

- 16th Euromicro Conference on Parallel, Distributed and Network-Based Processing (PDP 2008), IEEE, 2008, pp. 283–292.
- [56] E.-J. Im, K. Yelick, R. Vuduc, Sparsity: Optimization framework for sparse matrix kernels, *The International Journal of High Performance Computing Applications* 18 (1) (2004) 135–158.
 - [57] Y. Chen, G. Xiao, M. T. Ozsü, C. Liu, A. Y. Zomaya, T. Li, aeSpTV: An adaptive and efficient framework for sparse tensor-vector product kernel on a high-performance computing platform, *IEEE Transactions on Parallel and Distributed Systems* 31 (10) (2020) 2329–2345.
 - [58] R. Tian, L. Guo, J. Li, B. Ren, G. Kestor, A high-performance sparse tensor algebra compiler in Multi-Level IR, *arXiv preprint arXiv:2102.05187* (2021).
 - [59] S. Chou, S. Amarasinghe, Compilation of Dynamic Sparse Tensor Algebra, *Proc. ACM Program. Lang.* 6 (OOPSLA2) (Oct. 2022). doi:10.1145/3563338.
URL <https://doi.org/10.1145/3563338>
 - [60] A. Buluc, J. R. Gilbert, Challenges and advances in parallel sparse matrix-matrix multiplication, in: 2008 37th International Conference on Parallel Processing, IEEE, 2008, pp. 503–510.
 - [61] U. Borštnik, J. VandeVondele, V. Weber, J. Hutter, Sparse matrix multiplication: The distributed block-compressed sparse row library, *Parallel Computing* 40 (5-6) (2014) 47–58.
 - [62] Y. Niu, Z. Lu, H. Ji, S. Song, Z. Jin, W. Liu, TileSpGEMM: a tiled algorithm for parallel sparse general matrix-matrix multiplication on GPUs, in: *Proceedings of the 27th ACM SIGPLAN Symposium on Principles and Practice of Parallel Programming*, 2022, pp. 90–106.
 - [63] G. Ballard, A. Druinsky, N. Knight, O. Schwartz, Hypergraph partitioning for sparse matrix-matrix multiplication, *ACM Transactions on Parallel Computing (TOPC)* 3 (3) (2016) 1–34.
 - [64] N. Burkart, M. F. Huber, A survey on the explainability of supervised machine learning, *Journal of Artificial Intelligence Research* 70 (2021) 245–317.
 - [65] P. Sinha, Multivariate polynomial regression in data mining: methodology, problems and solutions, *Int. J. Sci. Eng. Res* 4 (12) (2013) 962–965.
 - [66] Y. M. Buckley, Generalised linear models, in: *Ecological Statistics*, Oxford University Press, 2014.
 - [67] T. Hastie, R. Tibshirani, Generalized Additive Models, *Statistical Science* 1 (3) (1986) 297 – 310. doi:10.1214/ss/1177013604.
URL <https://doi.org/10.1214/ss/1177013604>

- [68] H. Kokel, P. Odom, S. Yang, S. Natarajan, A unified framework for knowledge intensive gradient boosting: Leveraging human experts for noisy sparse domains, in: *Proceedings of the AAAI Conference on Artificial Intelligence*, Vol. 34, 2020, pp. 4460–4468.
- [69] W.-Y. Loh, *Classification and regression trees*, Wiley interdisciplinary reviews: data mining and knowledge discovery 1 (1) (2011) 14–23.
- [70] G. Singh, J. Gómez-Luna, G. Mariani, G. F. Oliveira, S. Corda, S. Stuijk, O. Mutlu, H. Corporaal, Napel: Near-memory computing application performance prediction via ensemble learning, in: *2019 56th ACM/IEEE Design Automation Conference (DAC)*, IEEE, 2019, pp. 1–6.
- [71] E. Ould-Ahmed-Vall, J. Woodlee, C. Yount, K. A. Doshi, S. Abraham, Using model trees for computer architecture performance analysis of software applications, in: *2007 IEEE International Symposium on Performance Analysis of Systems & Software*, IEEE, 2007, pp. 116–125.
- [72] B. Calder, D. Grunwald, M. Jones, D. Lindsay, J. Martin, M. Mozer, B. Zorn, Evidence-based static branch prediction using machine learning, *ACM Transactions on Programming Languages and Systems (TOPLAS)* 19 (1) (1997) 188–222.
- [73] A. Tousi, M. Luján, Comparative analysis of machine learning models for performance prediction of the SPEC benchmarks, *IEEE Access* 10 (2022) 11994–12011.
- [74] B. Bodin, L. Nardi, M. Z. Zia, H. Wagstaff, G. Sreekar Shenoy, M. Emani, J. Mawer, C. Kotselidis, A. Nisbet, M. Lujan, et al., Integrating algorithmic parameters into benchmarking and design space exploration in 3D scene understanding, in: *Proceedings of the 2016 International Conference on Parallel Architectures and Compilation*, 2016, pp. 57–69.
- [75] F. Hutter, H. H. Hoos, K. Leyton-Brown, Sequential model-based optimization for general algorithm configuration, in: *International conference on learning and intelligent optimization*, Springer, 2011, pp. 507–523.
- [76] M. Cianfriglia, F. Vella, C. Nugteren, A. Lokhmotov, G. Fursin, A model-driven approach for a new generation of adaptive libraries, *arXiv preprint arXiv:1806.07060* (2018).
- [77] D. Fenacci, B. Franke, J. Thomson, Workload characterization supporting the development of domain-specific compiler optimizations using decision trees for data mining, in: *Proceedings of the 13th international workshop on software & compilers for embedded systems*, 2010, pp. 1–10.
- [78] J. Bang, C. Kim, K. Wu, A. Sim, S. Byna, S. Kim, H. Eom, HPC workload characterization using feature selection and clustering, in: *Proceedings of the 3rd International Workshop on Systems and Network Telemetry and Analytics*, 2020, pp. 33–40.

- [79] M. Sato, Y. Ishikawa, H. Tomita, Y. Kodama, T. Odajima, M. Tsuji, H. Yashiro, M. Aoki, N. Shida, I. Miyoshi, et al., Co-design for A64FX manycore processor and” fugaku”, in: SC20: International Conference for High Performance Computing, Networking, Storage and Analysis, IEEE, 2020, pp. 1–15.
- [80] J. Xia, C. Cheng, X. Zhou, Y. Hu, P. Chun, Kunpeng 920: The first 7-nm chiplet-based 64-Core ARM SoC for cloud services, IEEE Micro 41 (5) (2021) 67–75.
- [81] A. W. S. (AWS), AWS Graviton3 (2022-01-23).
URL <https://aws.amazon.com/ec2/graviton/>
- [82] S. Rajamanickam, S. Acer, L. Berger-Vergiat, V. Dang, N. Ellingwood, E. Harvey, B. Kelley, C. R. Trott, J. Wilke, I. Yamazaki, Kokkos kernels: Performance portable sparse/dense linear algebra and graph kernels, arXiv preprint arXiv:2103.11991 (2021).
- [83] V. G. Reddy, Neon technology introduction, ARM Corporation 4 (1) (2008) 1–33.
- [84] N. Stephens, S. Biles, M. Boettcher, J. Eapen, M. Eyole, G. Gabrielli, M. Horsnell, G. Magklis, A. Martinez, N. Premillieu, et al., The ARM scalable vector extension, IEEE micro 37 (2) (2017) 26–39.
- [85] J. L. Greathouse, M. Daga, Efficient sparse matrix-vector multiplication on GPUs using the CSR storage format, in: SC’14: Proceedings of the International Conference for High Performance Computing, Networking, Storage and Analysis, IEEE, 2014, pp. 769–780.
- [86] P. A. Lane, J. D. Booth, Heterogeneous sparse matrix-vector multiplication via compressed sparse row format, Parallel Computing (2023) 102997.
- [87] I. Eo, W. Han, Y. Park, Roofline model and Profiling of HPC benchmarks, in: 2022 International Conference on Electronics, Information, and Communication (ICEIC), IEEE, 2022, pp. 1–4.
- [88] G. Flegar, H. Anzt, Overcoming load imbalance for irregular sparse matrices, in: Proceedings of the Seventh Workshop on Irregular Applications: Architectures and Algorithms, 2017, pp. 1–8.
- [89] D. Kim, J. Kim, Analysis of Several Sparse Formats for Matrices used in Sparse-Matrix Dense-Matrix Multiplication for Machine Learning on GPUs, in: 2022 13th International Conference on Information and Communication Technology Convergence (ICTC), IEEE, 2022, pp. 629–631.
- [90] M. Maggioni, T. Berger-Wolf, AdELL: An adaptive warp-balancing ELL format for efficient sparse matrix-vector multiplication on GPUs, in: 2013 42nd international conference on parallel processing, IEEE, 2013, pp. 11–20.

- [91] J. Chen, C. Xie, J. S. Firoz, J. Li, S. L. Song, K. Barker, M. Raugas, A. Li, MSREP: A Fast yet Light Sparse Matrix Framework for Multi-GPU Systems, arXiv preprint arXiv:2209.07552 (2022).
- [92] J. Willcock, A. Lumsdaine, Accelerating sparse matrix computations via data compression, in: Proceedings of the 20th annual international conference on Supercomputing, 2006, pp. 307–316.
- [93] A. C. De Melo, The new linux’perf’tools, in: Slides from Linux Kongress, Vol. 18, 2010, pp. 1–42.
- [94] J. Treibig, G. Hager, G. Wellein, Likwid: A lightweight performance-oriented tool suite for x86 multicore environments, in: 2010 39th international conference on parallel processing workshops, IEEE, 2010, pp. 207–216.
- [95] J. Dongarra, K. London, S. Moore, P. Mucci, D. Terpstra, Using PAPI for hardware performance monitoring on Linux systems, in: Conference on Linux Clusters: The HPC Revolution, Vol. 5, Linux Clusters Institute, 2001.
- [96] J. Eriksson, P. Ojeda-May, T. Ponweiser, T. Steinreiter, Profiling and tracing tools for performance analysis of large scale applications, PRACE: Partnership for Advanced Computing in Europe (2016) 1–30.
- [97] SuiteSparse Matrix Collection, <http://sparse.tamu.edu/>, accessed: 2023-01-19.
- [98] U. W. Pooch, A. Nieder, A survey of indexing techniques for sparse matrices, ACM Computing Surveys (CSUR) 5 (2) (1973) 109–133.
- [99] R. K. Brayton, F. G. Gustavson, R. A. Willoughby, Some results on sparse matrices, Mathematics of Computation 24 (112) (1970) 937–954.
- [100] B. Bollobás, C. Borgs, J. T. Chayes, O. Riordan, Directed scale-free graphs., in: SODA, Vol. 3, 2003, pp. 132–139.
- [101] B. Bollobás, B. Bollobás, Random graphs, Springer, 1998.
- [102] J. Oskarsson, P. Sidén, F. Lindsten, Scalable Deep Gaussian Markov Random Fields for General Graphs, in: International Conference on Machine Learning, PMLR, 2022, pp. 17117–17137.
- [103] C. R. Vogel, Computational methods for inverse problems, SIAM, 2002.
- [104] H. Zhao, T. Xia, C. Li, W. Zhao, N. Zheng, P. Ren, Exploring better speculation and data locality in sparse matrix-vector multiplication on intel xeon, in: 2020 IEEE 38th International Conference on Computer Design (ICCD), IEEE, 2020, pp. 601–609.

- [105] K. Kourtis, G. Goumas, N. Koziris, Optimizing sparse matrix-vector multiplication using index and value compression, in: Proceedings of the 5th conference on Computing frontiers, 2008, pp. 87–96.
- [106] T. Yokota, K. Ootsu, T. Baba, Potentials of branch predictors: From entropy viewpoints, in: International Conference on Architecture of Computing Systems, Springer, 2008, pp. 273–285.
- [107] J. R. Spirn, Program locality and dynamic memory management., Princeton University, 1973.
- [108] Y. Zhong, X. Shen, C. Ding, Program locality analysis using reuse distance, ACM Transactions on Programming Languages and Systems (TOPLAS) 31 (6) (2009) 1–39.
- [109] G. Keramidas, P. Petoumenos, S. Kaxiras, Cache replacement based on reuse-distance prediction, in: 2007 25th International Conference on Computer Design, IEEE, 2007, pp. 245–250.
- [110] C. Fox, D. Lojpur, A.-I. A. Wang, Quantifying temporal and spatial localities in storage workloads and transformations by data path components, in: 2008 IEEE International Symposium on Modeling, Analysis and Simulation of Computers and Telecommunication Systems, IEEE, 2008, pp. 1–10.
- [111] B. Bylina, J. Bylina, P. Stpiczynski, D. Szalkowski, Performance analysis of multicore and multinodal implementation of SpMV operation, in: 2014 Federated Conference on Computer Science and Information Systems, 2014, pp. 569–576. doi:10.15439/2014F313.
- [112] Z. Xie, G. Tan, W. Liu, N. Sun, IA-SpGEMM: An input-aware auto-tuning framework for parallel sparse matrix-matrix multiplication, in: Proceedings of the ACM International Conference on Supercomputing, 2019, pp. 94–105.
- [113] L. St, S. Wold, et al., Analysis of variance (ANOVA), Chemometrics and intelligent laboratory systems 6 (4) (1989) 259–272.
- [114] G. Biau, E. Scornet, A random forest guided tour, Test 25 (2016) 197–227.
- [115] R. E. Schapire, Explaining adaboost, Empirical Inference: Festschrift in Honor of Vladimir N. Vapnik (2013) 37–52.
- [116] T. Hastie, R. Tibshirani, J. Friedman, T. Hastie, R. Tibshirani, J. Friedman, Boosting and additive trees, The elements of statistical learning: data mining, inference, and prediction (2009) 337–387.
- [117] W. Jia, K. A. Shaw, M. Martonosi, Starchart: Hardware and software optimization using recursive partitioning regression trees, in: Proceedings of the 22nd international conference on Parallel architectures and compilation techniques, IEEE, 2013, pp. 257–267.

- [118] J. Poe, C.-B. Cho, T. Li, Using analytical models to efficiently explore hardware transactional memory and multi-core co-design, in: 2008 20th International Symposium on Computer Architecture and High Performance Computing, IEEE, 2008, pp. 159–166.
- [119] M. Letras, J. Falk, J. Teich, Decision tree-based throughput estimation to accelerate design space exploration for multi-core applications, in: MBMV 2021; 24th Workshop, VDE, 2021, pp. 1–11.
- [120] T. Fushiki, Estimation of prediction error by using K-fold cross-validation, *Statistics and Computing* 21 (2011) 137–146.
- [121] D. Berrar, Cross-Validation. (2019).
- [122] K. Polat, S. Güneş, Classification of epileptiform EEG using a hybrid system based on decision tree classifier and fast Fourier transform, *Applied Mathematics and Computation* 187 (2) (2007) 1017–1026.
- [123] R. E. Banfield, L. O. Hall, K. W. Bowyer, W. P. Kegelmeyer, A comparison of decision tree ensemble creation techniques, *IEEE transactions on pattern analysis and machine intelligence* 29 (1) (2006) 173–180.
- [124] L. Steiner, M. Jung, N. Wehn, Exploration of DDR5 with the Open-Source Simulator DRAMSys, in: MBMV 2021; 24th Workshop, 2021, pp. 1–11.
- [125] C. Alappat, J. Laukemann, T. Gruber, G. Hager, G. Wellein, N. Meyer, T. Wettig, Performance Modeling of Streaming Kernels and Sparse Matrix-Vector Multiplication on A64FX, in: 2020 IEEE/ACM Performance Modeling, Benchmarking and Simulation of High Performance Computer Systems (PMBS), IEEE, 2020, pp. 1–7.
- [126] M. Siracusa, V. Soria-Pardos, F. Sgherzi, J. Randall, D. J. Joseph, M. Moretó Planas, A. Armejach, A tensor marshaling unit for sparse tensor algebra on general-purpose processors, *MICRO '23*, Association for Computing Machinery, New York, NY, USA, 2023, p. 1332–1346. doi:10.1145/3613424.3614284. URL <https://doi.org/10.1145/3613424.3614284>
- [127] C. Zheng, S. Gu, T.-X. Gu, B. Yang, X.-P. Liu, BiELL: A bisection ELLPACK-based storage format for optimizing SpMV on GPUs, *Journal of Parallel and Distributed Computing* 74 (7) (2014) 2639–2647.
- [128] Z. Wang, T. Gu, PELLR: A Permutated ELLPACK-R Format for SpMV on GPUs, *Journal of Computer and Communications* 8 (4) (2020) 44–58.
- [129] I. Liiv, Seriation and matrix reordering methods: An historical overview, *Statistical Analysis and Data Mining: The ASA Data Science Journal* 3 (2) (2010) 70–91.

- [130] Ü. i. t. V. Çatalyürek, C. Aykanat, B. Uçar, On two-dimensional sparse matrix partitioning: Models, methods, and a recipe, *SIAM Journal on Scientific Computing* 32 (2) (2010) 656–683.
- [131] D. M. Pelt, R. H. Bisseling, A medium-grain method for fast 2D bipartitioning of sparse matrices, in: 2014 IEEE 28th International Parallel and Distributed Processing Symposium, IEEE, 2014, pp. 529–539.
- [132] P. Michaud, Best-offset hardware prefetching, in: 2016 IEEE International Symposium on High Performance Computer Architecture (HPCA), IEEE, 2016, pp. 469–480.
- [133] X. Yu, C. J. Hughes, N. Satish, S. Devadas, Imp: Indirect memory prefetcher, in: Proceedings of the 48th International Symposium on Microarchitecture, 2015, pp. 178–190.
- [134] F. Mantovani, M. Garcia-Gasulla, J. Gracia, E. Stafford, F. Banchelli, M. Josep-Fabrego, J. Criado-Ledesma, M. Nachtmann, Performance and energy consumption of HPC workloads on a cluster based on Arm ThunderX2 CPU, *Future generation computer systems* 112 (2020) 800–818.
- [135] A. Armejach, M. Casas, M. Moretó, Design trade-offs for emerging HPC processors based on mobile market technology, *J. Supercomput.* 75 (9) (2019) 5717–5740. doi:10.1007/s11227-019-02819-4.
- [136] A. Poenaru, T. Deakin, S. McIntosh-Smith, S. D. Hammond, A. J. Younge, An Evaluation of the Fujitsu A64FX for HPC Applications, in: Presentation in AHUG ISC 21 Workshop, 2021.
- [137] E. Calore, A. Gabbana, S. F. Schifano, R. Tripiccone, ThunderX2 performance and energy-efficiency for HPC workloads, *Computation* 8 (1) (2020) 20.
- [138] V. Soria-Pardos, A. Armejach, D. Suárez, M. Moretó, On the use of many-core Marvell ThunderX2 processor for HPC workloads, *The Journal of Supercomputing* 77 (2021) 3315–3338.
- [139] G. F. Oliveira, J. Gómez-Luna, L. Orosa, S. Ghose, N. Vijaykumar, I. Fernandez, M. Sadrosadati, O. Mutlu, DAMOV: A new methodology and benchmark suite for evaluating data movement bottlenecks, *IEEE Access* 9 (2021) 134457–134502.
- [140] A. Bean, N. Kapre, P. Cheung, G-DMA: improving memory access performance for hardware accelerated sparse graph computation, in: 2015 International Conference on ReConFigurable Computing and FPGAs (ReConFig), IEEE, 2015, pp. 1–6.
- [141] V. C. Cabezas, M. Püschel, Extending the roofline model: Bottleneck analysis with microarchitectural constraints, in: 2014 IEEE International Symposium on Workload Characterization (IISWC), IEEE, 2014, pp. 222–231.

- [142] B. Asgari, R. Hadidi, J. Dierberger, C. Steinichen, A. Marfatia, H. Kim, Copernicus: Characterizing the performance implications of compression formats used in sparse workloads, in: 2021 IEEE International Symposium on Workload Characterization (IISWC), IEEE, 2021, pp. 1–12.
- [143] J. Fowers, K. Ovtcharov, K. Strauss, E. S. Chung, G. Stitt, A high memory bandwidth fpga accelerator for sparse matrix-vector multiplication, in: 2014 IEEE 22nd Annual International Symposium on Field-Programmable Custom Computing Machines, IEEE, 2014, pp. 36–43.
- [144] P. Grigoras, P. Burovskiy, E. Hung, W. Luk, Accelerating SpMV on FPGAs by compressing nonzero values, in: 2015 IEEE 23rd Annual International Symposium on Field-Programmable Custom Computing Machines, IEEE, 2015, pp. 64–67.
- [145] C. Y. Lin, N. Wong, H. K.-H. So, Design space exploration for sparse matrix-matrix multiplication on FPGAs, *International Journal of Circuit Theory and Applications* 41 (2) (2013) 205–219.
- [146] Y. Umuroglu, M. Jahre, An energy efficient column-major backend for FPGA SpMV accelerators, in: 2014 IEEE 32nd International Conference on Computer Design (ICCD), IEEE, 2014, pp. 432–439.
- [147] T. Nguyen, C. MacLean, M. Siracusa, D. Doerfler, N. J. Wright, S. Williams, FPGA-based HPC accelerators: An evaluation on performance and energy efficiency, *Concurrency and Computation: Practice and Experience* 34 (20) (2022) e6570. [arXiv:https://onlinelibrary.wiley.com/doi/pdf/10.1002/cpe.6570](https://onlinelibrary.wiley.com/doi/pdf/10.1002/cpe.6570), doi:<https://doi.org/10.1002/cpe.6570>.
URL <https://onlinelibrary.wiley.com/doi/abs/10.1002/cpe.6570>
- [148] E. Nurvitadhi, A. Mishra, D. Marr, A sparse matrix vector multiply accelerator for support vector machine, in: 2015 International Conference on Compilers, Architecture and Synthesis for Embedded Systems (CASES), IEEE, 2015, pp. 109–116.
- [149] B. Asgari, R. Hadidi, T. Krishna, H. Kim, S. Yalamanchili, Alrescha: A lightweight reconfigurable sparse-computation accelerator, in: 2020 IEEE International Symposium on High Performance Computer Architecture (HPCA), IEEE, 2020, pp. 249–260.
- [150] K. Hegde, H. Asghari-Moghaddam, M. Pellauer, N. Crago, A. Jaleel, E. Solomonik, J. Emer, C. W. Fletcher, Extensor: An accelerator for sparse tensor algebra, in: Proceedings of the 52nd Annual IEEE/ACM International Symposium on Microarchitecture, 2019, pp. 319–333.
- [151] R. Hwang, T. Kim, Y. Kwon, M. Rhu, Centaur: A chiplet-based, hybrid sparse-dense accelerator for personalized recommendations, in: 2020 ACM/IEEE 47th Annual International Symposium on Computer Architecture (ISCA), IEEE, 2020, pp. 968–981.

- [152] A. K. Mishra, E. Nurvitadhi, G. Venkatesh, J. Pearce, D. Marr, Fine-grained accelerators for sparse machine learning workloads, in: 2017 22nd Asia and South Pacific design automation conference (ASP-DAC), IEEE, 2017, pp. 635–640.
- [153] E. Nurvitadhi, A. Mishra, Y. Wang, G. Venkatesh, D. Marr, Hardware accelerator for analytics of sparse data, in: 2016 Design, Automation & Test in Europe Conference & Exhibition (DATE), IEEE, 2016, pp. 1616–1621.
- [154] S. Pal, J. Beaumont, D.-H. Park, A. Amarnath, S. Feng, C. Chakrabarti, H.-S. Kim, D. Blaauw, T. Mudge, R. Dreslinski, Outerspace: An outer product based sparse matrix multiplication accelerator, in: 2018 IEEE International Symposium on High Performance Computer Architecture (HPCA), IEEE, 2018, pp. 724–736.
- [155] A. Parashar, M. Rhu, A. Mukkara, A. Puglielli, R. Venkatesan, B. Khailany, J. Emer, S. W. Keckler, W. J. Dally, SCNN: An accelerator for compressed-sparse convolutional neural networks, *ACM SIGARCH computer architecture news* 45 (2) (2017) 27–40.
- [156] E. Qin, A. Samajdar, H. Kwon, V. Nadella, S. Srinivasan, D. Das, B. Kaul, T. Krishna, Sigma: A sparse and irregular gemm accelerator with flexible interconnects for dnn training, in: 2020 IEEE International Symposium on High Performance Computer Architecture (HPCA), IEEE, 2020, pp. 58–70.
- [157] G. Zhang, N. Attaluri, J. S. Emer, D. Sanchez, Gamma: Leveraging Gustavson’s algorithm to accelerate sparse matrix multiplication, in: Proceedings of the 26th ACM International Conference on Architectural Support for Programming Languages and Operating Systems, 2021, pp. 687–701.
- [158] S. Zhang, Z. Du, L. Zhang, H. Lan, S. Liu, L. Li, Q. Guo, T. Chen, Y. Chen, Cambricon-X: An accelerator for sparse neural networks, in: 2016 49th Annual IEEE/ACM International Symposium on Microarchitecture (MICRO), IEEE, 2016, pp. 1–12.
- [159] Z. Zhang, H. Wang, S. Han, W. J. Dally, Sparch: Efficient architecture for sparse matrix multiplication, in: 2020 IEEE International Symposium on High Performance Computer Architecture (HPCA), IEEE, 2020, pp. 261–274.
- [160] X. Zhou, Z. Du, Q. Guo, S. Liu, C. Liu, C. Wang, X. Zhou, L. Li, T. Chen, Y. Chen, Cambricon-S: Addressing irregularity in sparse neural networks through a cooperative software/hardware approach, in: 2018 51st Annual IEEE/ACM International Symposium on Microarchitecture (MICRO), IEEE, 2018, pp. 15–28.

- [161] F. Sadi, J. Sweeney, T. M. Low, J. C. Hoe, L. Pileggi, F. Franchetti, Efficient SpMV operation for large and highly sparse matrices using scalable multi-way merge parallelization, in: Proceedings of the 52nd Annual IEEE/ACM International Symposium on Microarchitecture, 2019, pp. 347–358.
- [162] V. W. Lee, C. Kim, J. Chhugani, M. Deisher, D. Kim, A. D. Nguyen, N. Satish, M. Smelyanskiy, S. Chennupaty, P. Hammarlund, et al., Debunking the 100X GPU vs. CPU myth: an evaluation of throughput computing on CPU and GPU, in: Proceedings of the 37th annual international symposium on Computer architecture, 2010, pp. 451–460.